Journal Pre-proofs

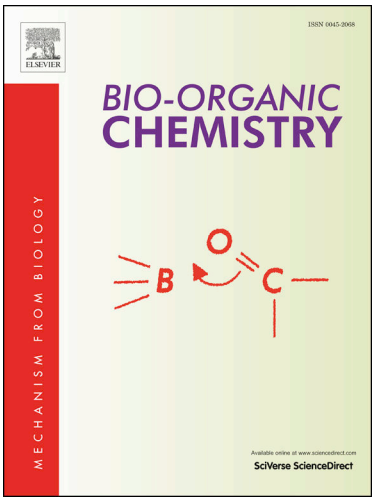

Ethyl benzoate bearing pyrrolizine/indolizine moieties: Design, synthesis and biological evaluation of anti-inflammatory and cytotoxic activities

Khalid M. Attalah, Ashraf N. Abdalla, Akhmed Aslam, Muhammad Ahmed, Mohammed A.S. Abourehab, Naser A. ElSawy, Ahmed M. Gouda

PII: S0045-2068(19)31501-9
DOI: https://doi.org/10.1016/j.bioorg.2019.103371
Reference: YBIOO 103371

To appear in: *Bioorganic Chemistry*

Received Date: 10 September 2019
Revised Date: 7 October 2019
Accepted Date: 16 October 2019

Please cite this article as: K.M. Attalah, A.N. Abdalla, A. Aslam, M. Ahmed, M.A.S. Abourehab, N.A. ElSawy, A.M. Gouda, Ethyl benzoate bearing pyrrolizine/indolizine moieties: Design, synthesis and biological evaluation of anti-inflammatory and cytotoxic activities, *Bioorganic Chemistry* (2019), doi: https://doi.org/10.1016/j.bioorg.2019.103371

Ethyl benzoate bearing pyrrolizine/indolizine moieties: Design, synthesis and biological evaluation of anti-inflammatory and cytotoxic activities

Khalid M. Attalah[1], Ashraf N. Abdalla[2,3], Akhmed Aslam[4], Muhammad Ahmed[2], Mohammed A.S. Abourehab[1,5], Naser A. ElSawy[6], Ahmed M. Gouda[7*]

[1]Department of Pharmaceutics, Faculty of Pharmacy, Umm Al-Qura University, Makkah 21955, Saudi Arabia;

[2]Department of Pharmacology and Toxicology, Faculty of Pharmacy, Umm Al-Qura University, Makkah 21955, Saudi Arabia;

[3]Department of Pharmacology, Medicinal and Aromatic plants research institute, National center for research, Khartoum 2404, Sudan;

[4]Department of Laboratory Medicine, Faculty of Applied Medical Sciences, Umm Al-Qura University, Makkah 21955, Saudi Arabia;

[5]Department of Pharmaceutics, Faculty of Pharmacy, Minia University, Minia 61519, Egypt;

[6]Department of Anatomy and Embryology, Faculty of Medicine, Zagazig University, Egypt;

[7]Department of Medicinal Chemistry, Faculty of Pharmacy, Beni-Suef University, Beni-Suef 62514, Egypt;

***Correspondence**

Ahmed M. Gouda: Department of Medicinal Chemistry, Faculty of Pharmacy, Beni-Suef University, Beni-Suef 62514, Egypt.

Scopus ID: 26321547200

ORCID: 0000-0003-4527-8885

Tel.: (002)-011-26897483

Fax: (002)-082-2317958

E-mail address: ahmed.gouda@pharm.bsu.edu.eg or amsaid@uqu.edu.sa

Graphical abstract

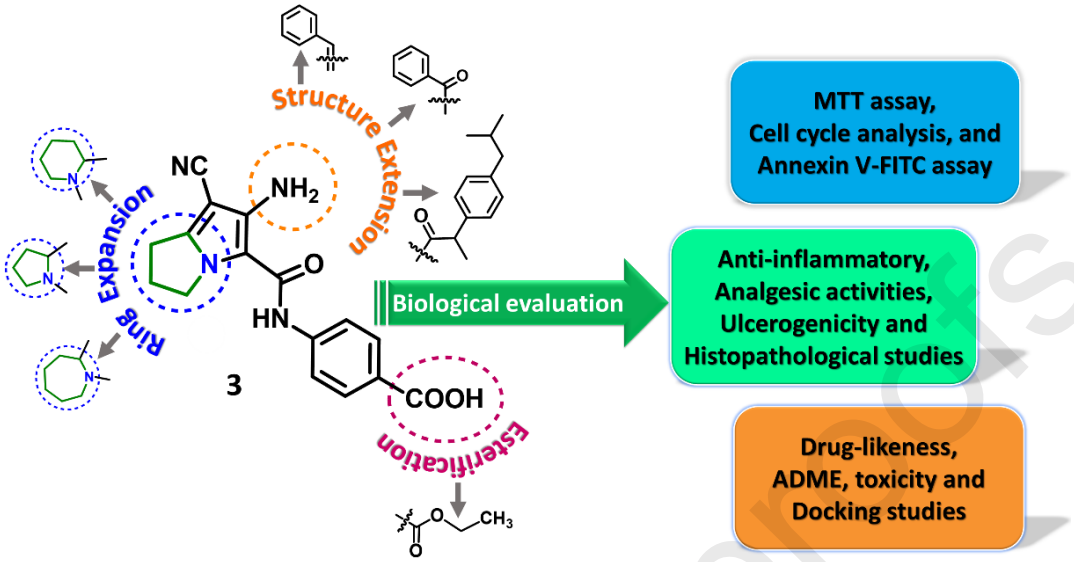

Highlights

1. Two new series of ethyl benzoate bearing pyrrolizine/indolizine moieties were synthesized.
2. The new compounds displayed anti-inflammatory and analgesic activities comparable to ibuprofen, mediated by COX-1/2 inhibition, with improved GIT safety profile.
3. The new compounds exhibited potent to moderate cytotoxicity against three (MCF-7, A2780 and HT29) cancer cell lines (IC_{50} = 0.02-23.35 µM).
4. Compound **9a** induced G1 cell cycle arrest and apoptosis in MCF-7 cells.
5. The new compounds exhibited nice fitting into COX-1/2 and drug-likeness scores comparable to licofelone and ketorolac.

Abstract

Two new series of ethyl benzoate bearing pyrrolizine and indolizine moieties **8-11** were synthesized and evaluated for their anti-inflammatory and anticancer activities. Among these derivatives, compounds **9a**, **10b** and **11b** displayed *in vivo* anti-inflammatory and analgesic activity comparable to ibuprofen. The acute ulcerogenicity and histopathological studies revealed better GIT safety profile than ibuprofen. Mechanistic study of these compounds revealed inhibitory activity against COX-1/2 with preferential inhibition of COX-2. Evaluation of cytotoxic activity of the new compounds using MTT assay revealed potent to moderate activity against three human (MCF-7, A2780 and HT29) cancer cell lines (IC_{50} = 0.02-23.35 μM). Compounds **9a**, **10a**,**b** and **11a**,**b** exhibited high cytotoxic selectivity against MCF-7 cells (SI = 4-84). Although the indolizine bearing derivatives **8-11b** exhibited higher selectivity to COX-2 than their corresponding pyrrolizine analogs **8-11a**, but they were less active and selective against MCF-7 cells. Cell cycle analysis and annexin V-FITC/PI assay revealed G1 cell cycle arrest and induction of apoptosis in MCF-7 cells by compound **9a**. The docking study revealed nice fitting of the new compounds into the active site of COX-1/2 with higher affinity to COX-2. Compounds **8-11** displayed drug-likeness score in the range of 0.67-1.56 compared to 1.06 for licofelone. These results suggested that compounds **9a**, **10b** and **11b** could be promising agents in future research as anti-inflammatory and anticancer agents.

Key words: pyrrolizine; indolizine; anti-inflammatory; cytotoxicity; cell cycle analysis; apoptosis.

1. Introduction

Cancer-related inflammation and pain are of the most common symptoms in solid tumors. They can be managed effectively with strong analgesic and anti-inflammatory agents [1,2]. Moreover, a huge volume of research describing the relationship between inflammation and cancer has been reported [3,4]. The upregulation of COX-2 gene was confirmed in several types of solid tumors such as breast [5], ovarian [6], and colon [7] cancers. The overexpression of COX-2 in cancer cells was associated with an increase in prostaglandin biosynthesis and inhibition of apoptosis [8]. Accordingly, it was not surprising that COX-2 inhibitors have antiproliferative activity against different types of cancer [9]. Most of the research in this area focused on selective COX-2 inhibitors, although selective COX-1 and nonselective COX inhibitors have also displayed potential anticancer activity [10,11]. However, the exact mechanism of action of these inhibitors is still unclear [9]. Moreover, the use of NSAIDs as chemopreventive or anticancer agents was restricted by many limitations such as GIT, kidney and cardiovascular side effects [12]. These problems encouraged the research to find new scaffolds with potential anti-inflammatory and anticancer activities.

Pyrrolizine is one of the promising scaffolds in this field. Several pyrrolizines **1-3** (**Fig. 1**) have displayed remarkable anti-inflammatory/anticancer activities [13-21]. Unlike other NSAIDs, the anti-inflammatory activity of licofelone **1** was associated with gastric sparing properties [14] and favorable cardiovascular profile [15]. The study of structure activity relationship (SAR) of licofelone **1** revealed that carboxylic acid and the two methyl groups are not essential for COX inhibition [13].

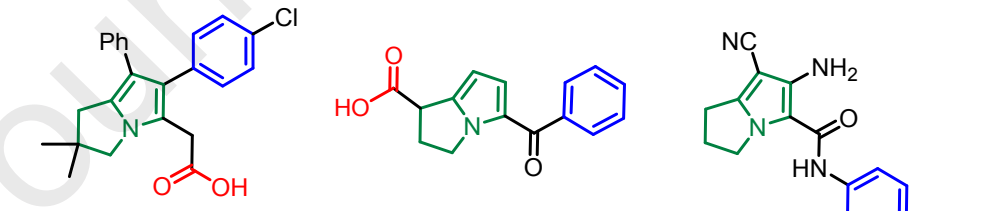

1 (Licofelone) — IC_{50} = **5.5** μM (MCF-7); IC_{50} = **4.7** μM (COX-2) [A1]

2 (Ketorolac) — IC_{50} = ~13 μM (A549) [A5]; IC_{50} = 140 nM (COX-2) [A5]

3

Fig.1. Pyrrolizine-based anti-inflammatory agents.

Licofelone **1** (**Fig. 1**) displayed also potent cytotoxic activity against breast, colon, and prostate cancer cell lines, mediated by induction of apoptosis [16-18]. This activity was mediated by the

induction of apoptosis in cancer cells. Licofelone **1** inhibited the growth of the MCF-7 breast cancer cells and COX-2 at nearly equal IC_{50} values [16,19]. These findings indicating that the two activities could be achieved simultaneously at the same dose level.

Ketorolac **2** (**Fig. 1**) is currently marketed as an analgesic and anti-inflammatory agent. Due to its potent analgesic activity, it was used as morphine sparing agent to alleviate cancer pain [20]. Moreover, ketorolac displayed potent anticancer activity against A549 cells with an IC_{50} value around 13 µM [21]. Moreover, compound **3** was previously reported with ~50% *in vivo* anti-inflammatory activity compared to ketorolac **2** [22]. Encouraged by these findings, compounds **3** was used as a lead compound in this study. Structural modifications of compound **3** were performed to investigate its anti-inflammatory and anticancer potential.

Rational Design

Esterification of the carboxylic acid group in NSAIDs was previously used to overcome their GIT toxicity [23]. Moreover, esterification of several NSAIDs was associated with improvement of their pharmacokinetic profile, cellular permeability and anticancer activity [21,23]. The ester derivatives of several NSAIDs have also displayed *in vitro* COX-1/2 inhibitory activity with high selectivity to COX-2 [24,25]. Based on these findings, we have designed two new series of nonacidic pyrrolizines and indolizine derivatives by masking the free carboxylic acid group and expansion of the pyrrolidine ring in in compound **3**, **Fig. 2**.

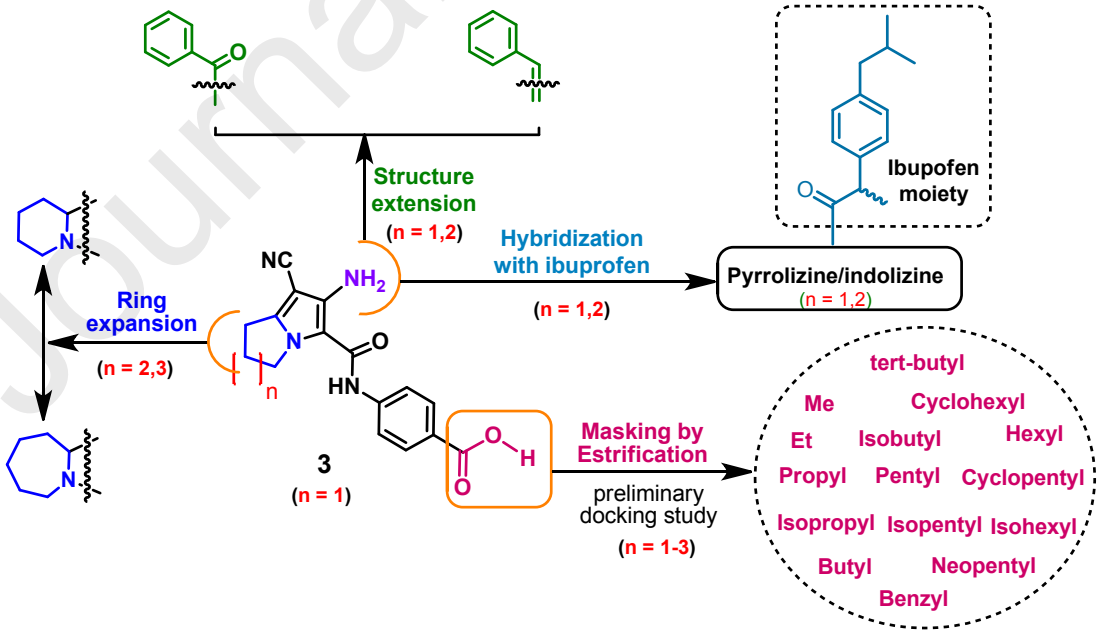

Fig. 2. Rational design of the new compounds.

A preliminary docking study was performed to evaluate binding affinity of seventeen ester derivatives of compound **3** toward COX-1/2 (Table S1, supplementary data). The results revealed high binding affinity toward COX-2 for the alkyl ester compared to compound **3**. Among these derivatives, the ethyl ester displayed the highest affinity to COX-2. The results also revealed an increase in COX-2 selectivity on expansion of the pyrrolidine ring in compound **3** to piperidine ring. On the other hand, expansion of pyrrolizine to azepine ring was associated with a noticeable increase in binding affinity to COX-1, suggesting that the resulting pyrroloazepine would be a nonselective COX inhibitor.

To improve dinging affinity of the new compounds toward COXs, extension of the chemical structure of ethyl ester of compound **3** and its indolizine analog was considered. Both benzoyl and benzylidene groups which can form additional hydrophilic/hydrophobic interactions with COXs were selected for this study. Based on the structural difference between the two COXs, increasing the molecular volume by benzoyl or benzylidene moieties could be used to increase selectivity to COX-2 [24]. The preliminary docking study revealed higher affinity for benzoyl or benzylidene derivatives toward COX-1/2 compared to compound **3** (Table S2, supplementary data).. Moreover, hydrides of aryl propionic acid derived NSAIDs with pyrrolizines have proven high safety in GIT. In this study we have designed two hybrids of ibuprofen with pyrrolizine/indolizine to compare their anti-inflammatory and anticancer activities, **Fig. 2**.

2. Results and discussion

2.1. Chemistry:

Synthesis of the starting materials was outlined in **Scheme 1**. Compounds **5a-c** and **7** were synthesized according to the previous reports [26-28]. Moreover, compound **8a** was prepared from the reaction of 2-(pyrrolidin-2-ylidene)malononitrile **5a** with ethyl 4-(2-chloroacetamido)benzoate **7** in acetone according to our previous report [29].

Similarly, compounds **8b**,**c** were obtained from the reaction of compound **7** with 2-(piperidin-2-ylidene)malononitrile **5b** and 2-(azepan-2-ylidene)malononitrile **5c**, respectively. The two compounds were prepared using the same reaction conditions applied for preparation of compound **8a**, **Scheme 1**. The expected mechanisms of cyclization of pyrrolizine and indolizine nuclei were previously discussed [27,30]. The expected mechanism of cyclization of the

pyrroloazepine **8c** is essentially similar to those of pyrrolizine and indolizine derivatives **8a**,**b**. The reaction can take place in two steps. The first step involves dehydrohalogenation catalyzed by potassium carbonate. The second step involves intramolecular cyclization to give pyrroloazepine **8c**. The spectral data are provided in supplementary data (Fig. S1-91).

The IR spectrum of compound **8b** revealed absorption band at 2211 cm^{-1} assigned for cyano group and two stretching bands at 1699 and 1672 cm^{-1} attributed to carbonyl groups. The ^{1}H NMR spectrum of compound **8b** revealed four signals at δ 1.76-4.11 ppm attributed to protons of the four methylene ($C\underline{H}_2$) groups of indolizine nucleus, a singlet signal at δ 5.35 ppm attributed to the two protons of amino ($N\underline{H}_2$) group and two doublet signals were observed at δ 7.70-7.91 ppm, indicating protons of the *para*-substituted phenyl ring of compound **8b**. Moreover, a singlet signal was observed at δ 9.82 ppm indicating the amide proton (CON<u>H</u>).

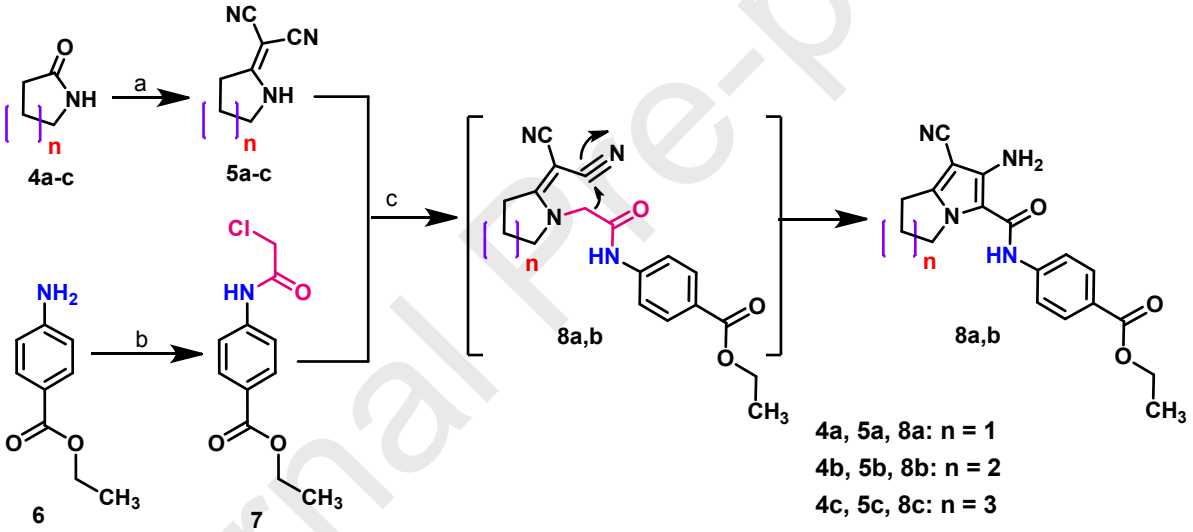

Scheme 1. Reagents and conditions: (a) $(CH_3)_2SO_4$, benzene, $CH_2(CN)_2$; b) $ClCH_2COCl$, g. acetic acid, CH_2COONa, rt, 2 h; (c) acetone, K_2CO_3, reflux (50-60 °C), 24 h.

The ^{13}C NMR spectrum of compound **8b** revealed a signal at δ 14.71 ppm due to the methyl ($\underline{C}H_3$) group carbon. Four signals were observed at δ 19.00-45.84 ppm attributed to carbons of the four methylene ($\underline{C}H_2$) groups of indolizine nucleus. Another signal at δ 60.84 ppm indicated the methylene ($\underline{C}H_2$) group carbon of ethyl side chain. Moreover, two signals at δ 159.85 and 165.90 ppm attribute to amide and ester group carbons, respectively. DEPT C^{135} spectrum of compound **8b** revealed two signals (up) at δ 119.41 and 130.49 indicating the aromatic <u>C</u>H

groups. Mass spectra of compound **8b** revealed the molecular ion peak at m/z = 351 ($[M-H]^+$, 100%)

The IR spectrum of compound **8c** revealed absorption band at 2212 cm^{-1} assigned for cyano group and two stretching bands at 1706 and 1667 cm^{-1} attributed to carbonyl groups. The ^1H NMR spectrum revealed a triplet signal at δ 1.28 ppm and singlet signal at δ 4.62 ppm attributed to methyl ($C\underline{H}_3$) and amino ($N\underline{H}_2$) groups. Two doublet signals at δ 7.73 and 8.01 ppm indicated aromatic protons of the *para*-substituted phenyl ring. One singlet signal at δ 10.35 ppm assigned for the amide proton (CON<u>H</u>). The ^{13}C NMR spectrum of compound **8c** revealed five signals at δ 26.21-47.27 ppm attributed to the five methylene ($\underline{C}H_2$) groups carbons of the azepine ring. Moreover, two signals at δ 159.23 and 165.64 ppm attribute to amide and ester group carbons, respectively. DEPT C^{135} spectrum of compound **8c** revealed two signals (up) at δ 118.98 and 129.29 indicating the aromatic <u>C</u>H group carbons. Mass spectra of compound **8c** revealed the molecular ion peak at m/z = 365 (M^+-H, 100%).

Compound **8c** was obtained in poor yield (36%) compared to 62 and 54% for compounds **8a** and **8b**, respectively. Moreover, the results of the preliminary docking study suggested that compound **8c** will have approximately equal affinity to COX-1/2. Accordingly, this work focused mainly on derivatization of compounds **8a**,**b**.

The Schiff bases **9a**,**b** were obtained by refluxing compounds **8a,b** with benzaldehyde, **Scheme 2**. The IR spectra revealed an absorption band at 2218 and 2211 cm^{-1} assigned to the cyano groups in compounds **9a** and **9b**, respectively. The absorption bands of the two carbonyl groups appeared in the ranges of 1672-1714 cm^{-1}. The ^1H NMR spectra of compounds **9a**,**b** revealed the appearance of new singlet signals at δ 9.13 and 9.15 ppm attributed to the benzylidene protons (PhC<u>H</u>=N). The aromatic protons of the benzylidene moiety appeared at the range of δ 7.51-8.04 ppm. Moreover, ^{13}C NMR spectra revealed three signals at the range of δ 158.61-166.23 ppm attributed to the benzylidene (Ph<u>C</u>H=N), amide (<u>C</u>ONH) and ester (<u>C</u>OOEt) group carbons. DEPT C^{135} spectra of compounds **9a**,**b** revealed five signals (up) at δ 118.68-132.76 ppm attributed to aromatic (<u>C</u>H) carbons. Mass spectra of compounds **9a**,**b** revealed the molecular ion peaks at m/z = 426 (M^+) and 439 ($[M-H]^+$), respectively.

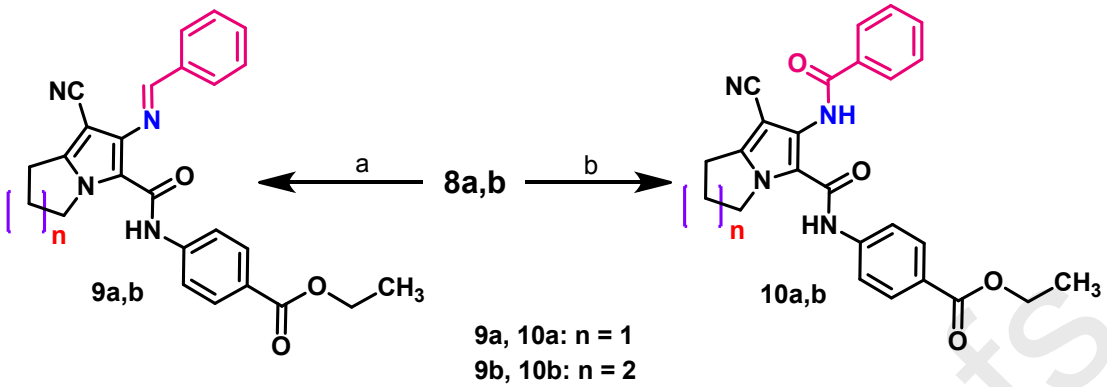

Scheme 2. Reagents and conditions: (a) benzaldehyde, absolute ethanol, g. acetic acid, reflux 6 h (70-80 °C); (b) benzoyl chloride, K_2CO_3, DCM, stir, rt, 24 h.

The amide derivatives **10a**,**b** were obtained by benzoylation of compounds **8a**,**b**, **Scheme 2**. The IR spectra of compounds **10a**,**b** revealed a stretching band at 2220 and 2221 cm^{-1} assigned to cyano groups in compounds **10a** and **10b**, respectively. Two stretching band at the range of 1651-1717 cm^{-1} attributed to the carbonyl groups of the two compounds. The ^1H NMR spectra of compounds **10a**,**b** revealed two signals at the range δ 7.99-10.24 ppm attributed to the two amide protons (Ph-NHCO and Ph-CONH). The ^{13}C NMR spectra showed three signals at δ 157.69-169.59 ppm attributed to carbonyl carbons of the two amide (CONH) and ester (COOEt) groups. DEPT C^{135} spectra of five signals (up) at the range of δ 118.62-133.36 ppm attributed to the aromatic (CH) carbons. Mass spectra of compounds **10a,b** revealed the molecular ion peaks at m/z = 456 $[(M+CH_3)-1]^+$ and 455 $([M-H]^+)$, respectively.

The hybrids **11a**,**b** were prepared from the reaction of the acid chloride of ibuprofen with compounds **8a**,**b**, **Scheme 3**. The IR spectrum of hybrids revealed absorption band at 2222 cm^{-1} assigned to cyano groups and two stretching bands at the range of 1667-1724 cm^{-1} attributed to the carbonyl groups.

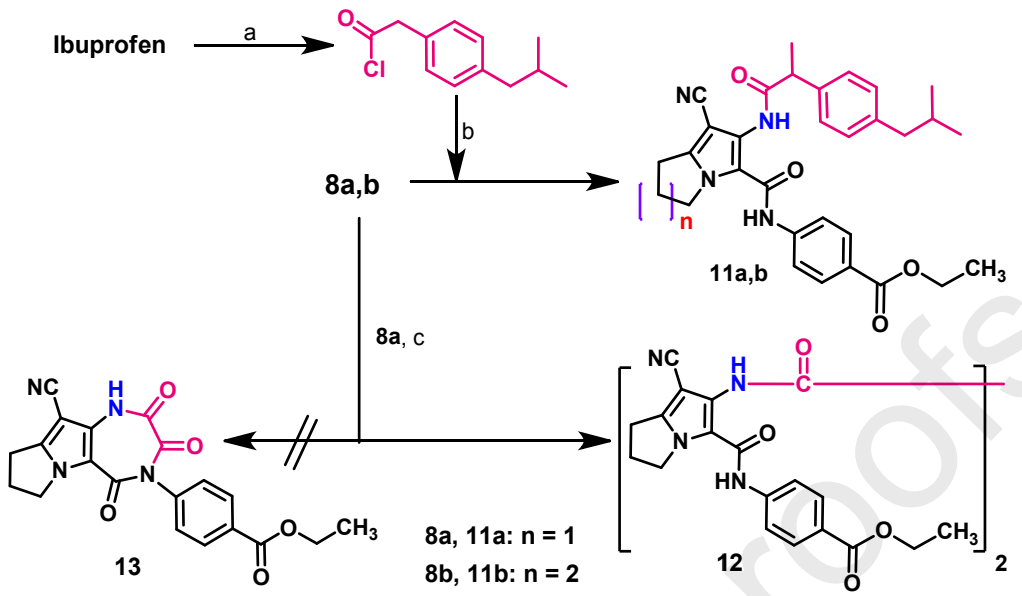

Scheme 3. Reagents and conditions: (a) $SOCl_2$, heat (70-80 °C), 2 hr; (b) DCM, K_2CO_3, stir, rt, 24 h; (c) oxalyl chloride, DCM, stir, rt, 4 hr.

The ^{1}H NMR spectra of compounds **11a**,**b** revealed the appearance of doublet signal at δ 0.78 and 0.88 ppm attributed to the two methyl ($CH(\underline{CH_3)_2}$) groups of isobutyl moiety. Two new doublets at δ 6.97-7.27 ppm were observed indicated the aromatic protons of the *p*-substituted phenyl ring of ibuprofen moiety. Moreover, two singlet signals were observed at the range of δ 7.39-10.26 ppm attributed to the amide protons. The ^{13}C NMR spectra showed three signals at the range of 157.74-177.51 ppm attributed to the three carbonyl carbons. DEPT C^{135} spectra of compounds **11a**,**b** revealed five new signals at δ 18.09-49.76 ppm indicated the aliphatic carbons of ibuprofen moiety. Moreover, two new signals at the range of δ 127.40-129.98 ppm attributed to the CH groups of the *para*-substituted phenyl of ibuprofen moiety. Mass spectra of compounds **11a**,**b** revealed the molecular ion peaks at m/z = 525 $[M^+-H]^+$ and 554 $[(M+CH_3)-1]^+$, respectively.

Moreover, the tricyclic diazepino[5,6-b]pyrrolizine **13** was also evaluated in the preliminary docking study for its binding affinity to COX-1/2. The results of this study revealed high potential selectivity toward COX-2 (Table S2, supplementary data). In attempt to prepare the tricyclic diazepino[5,6-b]pyrrolizine **13**, oxalyl chloride was reacted with compound **8a** in DCM, **Scheme 3**. Unfortunately, the reaction failed to give the expected product **13**. Instead, a dimeric product **12** was obtained which exhibited bad solubility in most of organic solvents. Due to its

poor physical properties and the high molecular weight, compound **12** was excluded form biological evaluation.

The IR, spectrum of compound **12** revealed a stretching band at 2210 cm^{-1} assigned to cyano group and two absorption band at 1667, 1707 cm^{-1} attributed to carbonyl groups. The ^{1}H NMR spectrum revealed two singlet signals at δ 9.87 and 10.78 ppm attributed to the two amide protons. The ^{13}C NMR spectrum of compound **12** revealed three signals at δ 158.14, 161.69 and 165.80 ppm attributed to the carbonyl carbons of amide, ester and oxalyl groups, respectively. DEPT C^{135} spectrum revealed δ 119.81 and 130.59 ppm indicated the aromatic CH groups of the *para*-substituted phenyl rings. Mass spectrum revealed the molecular ion at m/z = 731 ($[M+H]^{+}$).

2.2. Biological evaluation

2.2.1. Anti-inflammatory activity

Compounds **8-11** were evaluated for their *in vivo* anti-inflammatory activity using carrageenan induced rat paw edema model [31]. According to this model, inhibition in carrageenan-induced inflammation after treatment with the new compounds was used as a measure of their anti-inflammatory activity. The test compounds and the reference drug (ibuprofen) were given orally to Sprague Dawley rats at a dose of 0.48 mmol/kg. Results were outlined in **Fig. 3**.

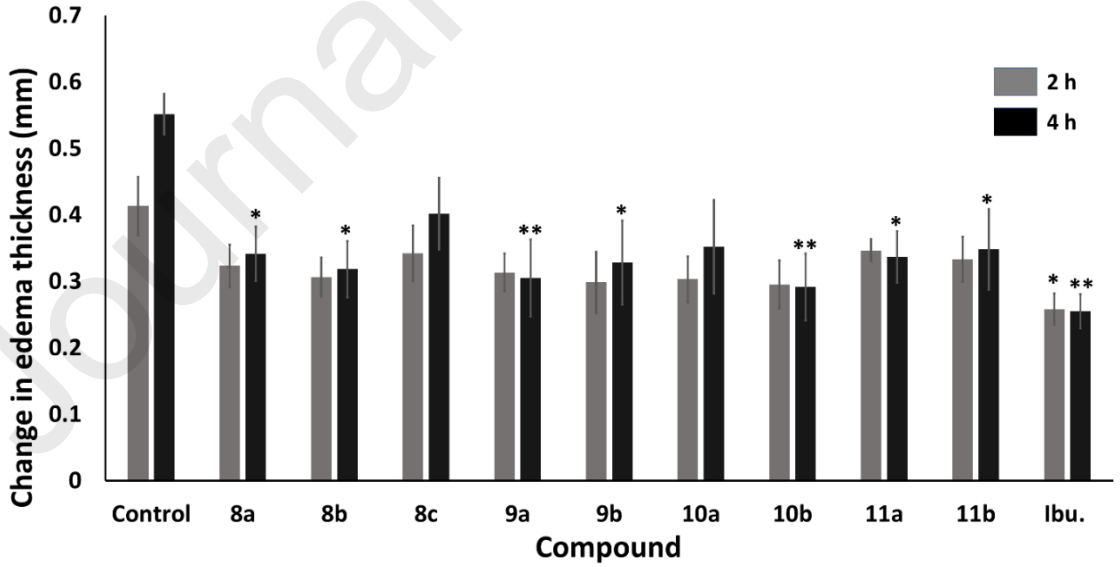

Fig. 3. Change in rat paw edema thickness at 2h and 4h post-carrageenan injection; data expressed as mean ± SEM, (n = 6); data were analyzed by One way ANOVA followed by Dunnett Multiple Comparisons Test; * statistically significant from control (P <0.05), ** statistically significant from control (P <0.01).

The anti-inflammatory activity of the new compounds was calculated according to our previous report [30]. The results were summarized in **Table 1**. The new compounds displayed 17.33-28.62% inhibition of inflammation compared to 37.49% for ibuprofen at 2h post-carrageenan injection. The activity was increased to 27.19-46.32% anti-inflammatory activity (4 h post-carrageenan injection), compared to 53.78% anti-inflammatory activity for ibuprofen, **Table 1**.

Compounds **8a-c** displayed 27.19-42.30% inhibition of inflammation (4h post-carrageenan injection), where compound **8b** was the most active. On the other hand, compounds **9a**,**b** and **10a**,**b** exhibited better anti-inflammatory activity (36.26-46.32%) than the parent compounds **8a,b**. Compounds **11a**,**b** showed delayed anti-inflammatory activity, which reached 38.03% for the pyrrolizine derivative **11a**. Among the new compounds, the benzoyl derivative **10b** was the most active while compound **8c** exhibited the lowest anti-inflammatory activity.

Table 1. Anti-inflammatory activity of compounds **8-11** and ibuprofen.

Comp. No	Anti-inflammatory activity (%) [a]		Ulcer index [b]
	2h	4h	
Control	-	-	-
8a	21.77	38.07	2.76
8b	25.80	42.30	4.66
8c	**17.33**	**27.19**	nt
9a	24.19	44.72	5.83
9b	27.82	40.49	2.99
10a	26.61	36.26	5.43
10b	**28.62**	**46.32**	4.99
11a	16.12	38.03	0
11b	19.35	35.89	0
Ibu.	**37.49**	**53.78**	10.96

[a] Anti-inflammatory activity = 100 x (1-L_t/L_c); L_t is the mean change in paw thickness in rats treated with tested compounds/ibuprofen (Ibu.); L_c is the mean increase in paw thickness in rats treated with vehicle;
[b] sum of %incidence of ulcers/10, average number of ulcers and average severity of ulcers; (n = 6), nt, not tested.

Generally, the new compounds **8-11** exhibited moderate to strong anti-inflammatory activity. The degree of inhibition in edema thickness were statistically significant from control for most of the

new compounds at 4h. The delayed anti-inflammatory activity of these compounds could be due to pharmacokinetic issues.

2.2.2. Analgesic activity

2.2.2.1. Hot plate test

The new compounds were evaluated for their analgesic activity against thermal pain using hot plate test according to the previous reports [26,30]. The latency time was determined at 2h and 4h after administration of test compounds and ibuprofen (0.48 mmol/kg p.o.). The extension in withdrawal latency was taken as an index for analgesic effect. The results were summarized in **Table 2**.

The results revealed the ability of compound **8b** to increase pain reaction time to 14.25 sec after 4 h in comparison with its control. This result was significant and comparable to ibuprofen (14.18 sec), **Table 2**. Moreover, compounds **9a** and **11a** increased pain reaction time after 4h to 13.40 and 13.42 sec, respectively. However, ibuprofen showed better effects than both compounds **9a** and **11a**.Treatment with compound **10b** increased pain reaction time to 15.30 sec after 2 h, which persisted after 4 h (15.10 sec). In addition, compound **11b** increased pain reaction time to 15.10 sec.

Table 2. Analgesic effects of compounds **8-11** and ibuprofen using hot plate test.

Comp. No	Latency time ± SEM		
	0h	2h	4h
Control	8.75±0.35	8.07±0.37	8.30±0.75
8a	8.45±0.61	10.32±0.33	12.62±1.32
8b	8.71±0.57	11.23±0.64	14.25±1.43**
8c	8.15±0.53	9.35±0.55	9.68±0.75
9a	8.73±0.71	11.33±1.18	13.40±1.68*
9b	8.08±0.72	11.25±0.99	11.90±1.20
10a	8.83±0.73	10.85±1.13	9.88±1.03
10b	8.72±0.93	**15.25±1.44****	**15.30±1.23****
11a	8.74±0.54	9.92±1.07	13.42±1.23*
11b	8.72±0.74	**10.55±1.31**	**15.10±1.31****
Ibu.	8.72±0.39	11.85±0.39*	14.18±1.28*

Data were represented as means ± SEM, n = 6; data were analyzed by One way ANOVA followed by Dunnett Multiple Comparisons Test; * statistically significant from control (P <0.05), ** statistically significant from control (P <0.01).

Compounds **8a**, **9b** and **10a** increased the reaction time, although these changes were not significant compared to control. These results revealed that the new compounds **8b**, **9a**, **10b** and **11a**,**b** have analgesic activity comparable to or slightly higher than ibuprofen.

2.2.2.2. Acetic acid-induced writhing test

The analgesic activity of the new compounds **8-11** were also evaluated by acetic acid induced writhing test [22]. After treatment with test compounds, the decrease in number of acetic acid-induced writhes compared to control was used as a measure of analgesic activity. The ability of the test compounds to inhibit induced writhes was calculated in **Table 3**.

The results revealed 29.74-51.54% inhibition of acetic acid-induced writhes by test compounds **8-11**, compared to 62.33% for ibuprofen. Compounds **9a** and **10b** exhibited 50.44% and 51.54% inhibition of abdominal writhes, respectively. Moreover, compound **11b** displayed 47.58% inhibition of the induced writhes which was higher than the parent compound **8b**.

Table 3. Analgesic activity of compounds **8-11** and ibuprofen using acetic acid-induced writhing test.

Comp. No	Writhing reflex ± SEM	Inhibition %
Control	75.67±6.30	-
8a	47.50±4.06**	37.22
8b	43.50±4.62**	42.51
8c	53.17±5.62*	29.74
9a	37.50±5.72**	**50.44**
9b	46.00±4.52**	39.21
10a	51.17±5.91**	32.38
10b	36.67±5.84**	**51.54**
11a	42.50±4.37**	43.83
11b	39.67±2.59**	**47.58**
Ibu.	28.50±2.73**	62.33

Data expressed as mean number of writhes ± SEM; %Inhibition of abdominal writhes = 100*[(n – n′)/n], where n is mean number of writhes in control group, n′ is the mean number of writhes in test group; data were analyzed by One way ANOVA followed by Dunnett Multiple Comparisons Test; * statistically significant from control ($P < 0.05$), ** statistically significant from control ($P < 0.01$).

2.2.3. Acute ulcerogenicity studies

GIT toxicity is one of the major side effects of NSAIDs [12]. In this work, compounds **8-11** were evaluated for their GIT side effects. The ulcerogenic liability of these compounds was evaluated according to the previous report [22]. The test compounds **8-11** and ibuprofen were given to the rats at a dose of 0.48 mmol/kg/day p.o. for 3 days. In the fourth day, the rats were sacrificed, and their stomachs were removed and examined for any mucosal damage using magnifying lens (10x). Number of mucosal damage (red spots) were counted and their severity were graded from 0-4, where 0 for normal (no lesion) and 4 for severe lesions (Table S4, supplementary data). Ulcer index was calculated for each of the tested compounds according to the previous report [22]. The results were summarized in **Table 1**.

Examination of stomachs of control group revealed normal texture with no ulcerative spots. In addition, only small to wide red spots were observed in the stomachs of rats treated with test compounds **8-10** with no ulcerative spots. Stomachs of the rats treated with ibuprofen revealed several spots ranging from hyperemia to slight injury. Compound **9b**, which showed the highest selectivity towards COX-2, displayed low ulcer index (2.99), compared to 10.96 for ibuprofen. On the other hand, stomachs of the rats treated with compounds **11a**,**b** showed normal stomach texture, **Table 1**.

2.2.4. Histopathological studies

To investigate the effects of the test compounds on histological structure of gastric wall, cross sections in stomachs used in acute ulcerogenicity study were examined microscopically. These sections were examined after staining with hematoxylin and eosin (H and E) according to the previous report [26]. The results were presented in **Figs. 4** and **5**.

Stomach cross sections of the stomachs of control rats (received vehicle) showed normal histological structure of gastric layers, while those treated with ibuprofen showed abnormal histological structure of gastric layers with sloughing of gastric mucosa, **Figs. 4** and **5**.

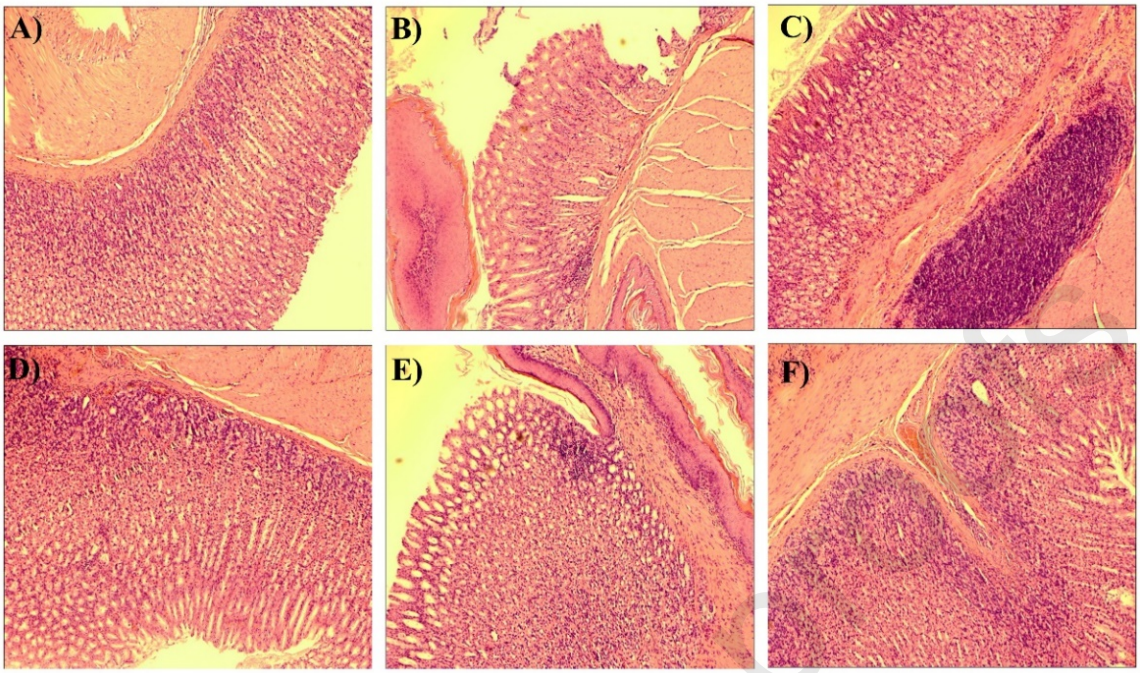

Fig. 4. Cross section of stomach of a rat (H & E stain X 100) treated with A) vehicle (control); B) ibuprofen; C) compound **8a**; D) compound **8b**; E) compound **9a**; F) compound **9b**.

The cross sections of stomachs of rats treated with compound **8a** showed normal histological structure of gastric mucosa with focal lymphocytic infiltration, while those treated with compound **8b** showed also normal histological structure of gastric mucosa with some change in submucosa.

Histopathological examination of cross sections of stomachs of rats treated with compound **9a** showed normal histological structure of gastric mucosa with some change in submucosa specially at gastroesophageal junction. In addition, the cross sections of stomachs of the rats treated with compound **9b** showed normal histological structure of gastric mucosa with some change in submucosa. Moreover, the cross sections of stomach of rats treated with compounds **10a,b** showed normal histological structure of gastric mucosa with some change in submucosa, while those treated with compounds **11a**,**b** showed normal histological structure of gastric layers.

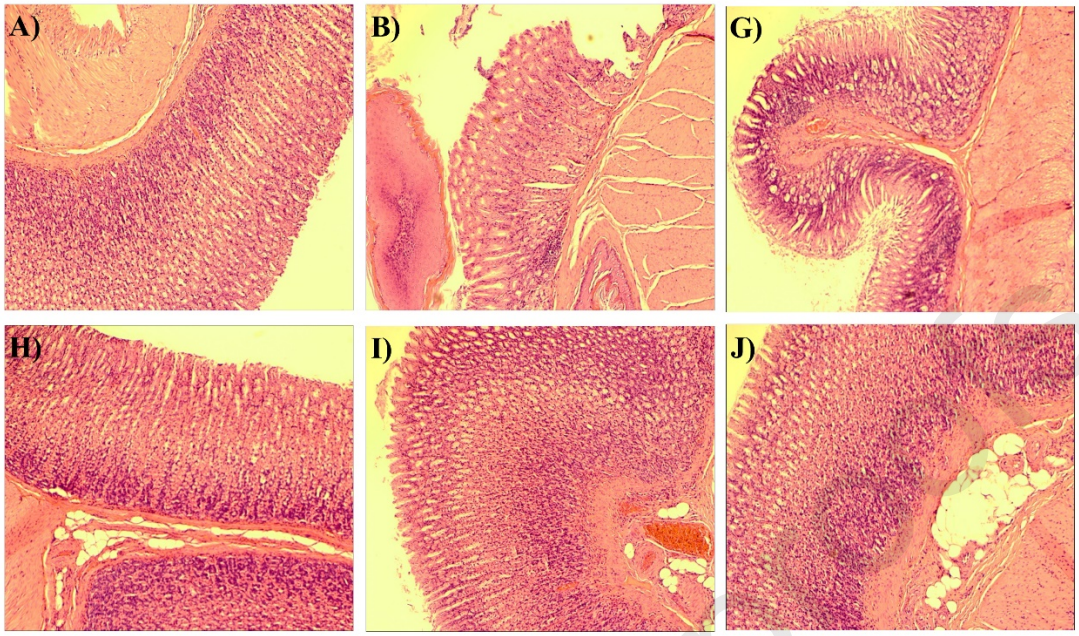

Fig. 5. Cross section of stomach of a rat (H & E stain X 100) treated with A) vehicle (control); B) ibuprofen; G) compound **10a**; H) compound **10b**; I) compound **11a**; J) compound **11b**.

2.2.5. COX-1/2 inhibitory activity

The mechanism of the anti-inflammatory activity of the pyrrolizine derivatives **1** and **2** was mediated by COX inhibition [14,21]. In this work, compounds **8-10** were evaluated for their COX-1/2 inhibitory activity. The assay was performed according to the previous report [32]. The results expressed in IC_{50} values and selectivity indices (SIs) were summarized in **Table 4**.

The tested compounds displayed inhibitory activity against COX-1 (IC_{50} = 5.52-63.85 µM), and COX-2 (IC_{50} = 1.46-11.57 µM). Compounds **8a-c** exhibited inhibitory activity against the two COXs with preferential inhibition of COX-2 (SI = 3.69-8.65), where the indolizine analog **8b** was the most selective toward COX-2. Although compounds **8a** and **8c** showed nearly equal selectivity for the two COXs, but compound **8a** was nearly eight times more potent as COX-2 inhibitor.

Compounds **9a,b** were less active in inhibiting COX-1 than their parent compounds **8a**,**b**. As a result their selectivity to COX-2 was markedly improved compared to the parent compounds. Among the tested derivatives, compound **9b** was the most selective to COX-2 (SI = 27.52). Moreover, the benzoyl derivatives **10a,b** showed better COX-2 inhibitory activity than their corresponding Schiff bases **9a,b**. Compound **10a** showed twofold increase in SI compared to **9a**, **Table 4**.

Table 4. COX-1/2 inhibitory activity of compounds **8-10**, celecoxib and indomethacin.

Comp. No	IC_{50} (μM) [a]		SI [b]
	COX-1	COX-2	
8a	5.52±0.24	1.46±0.51	3.78
8b	37.52±1.92	4.34±0.317	8.65
8c	22.75±3.64	11.57±0.526	3.69
9a	37.20±2.09	6.89±0.33	5.40
9b	63.85±6.52	2.32±0.25	27.52
10a	35.44±0.26	3.754±0.42	9.44
10b	28.31±0.84	2.146±0.79	13.19
Celecoxib	43.03±3.54	0.579±0.08	74.32
Indomethacin	1.25±0.07	64.76±3.72	0.02

[a] Values represent the mean of four determinations ± SEM, (n = 3).
[b] selectivity index (*SI*) for COX-2 = IC_{50} against COX-1/IC_{50} against COX-2.

2.2.6. Cytotoxic activity

2.2.6.1. Cytotoxicity assay

Beside their anti-inflammatory activities, licofelone **1** and ketorolac **2** exhibited remarkable cytotoxic activity against different types of solid tumors [16-19,21]. Encouraged by these findings, compounds **8-11** were investigated for their cytotoxicity against different human organ cancer cell lines, including breast (MCF-7), ovarian (A2780) and colon (HT29) cancer cell lines. The three cancer cell lines were selected based on the reported anticancer activity of licofelone [16-18]. The 3-(4,5-dimethylthiazol-2-yl)-2,5-diphenyl-2*H*-tetrazolium bromide (MTT) assay was used in the evaluation of cytotoxic activity of these compounds according to our previous reports [34,35]. The results were represented in **Table 5**. The resulted revealed potent to moderate cytotoxic activities for the new compounds against the three cancer cell lines with IC_{50} values in the range of 0.02-23.35 μM, compared to lapatinib (IC_{50} = 6.80-12.67 μM). Among these derivatives, compound **9a** displayed the highest cytotoxic activity against MCF-7 (IC_{50} = 0.02 μM) cell line, while compound **11b** was the most active against A2780 and HT29 cells.

Table 5. IC_{50} values of compounds **8-11** and lapatinib against MCF-7, A2780, HT29 and MRC5 cell lines

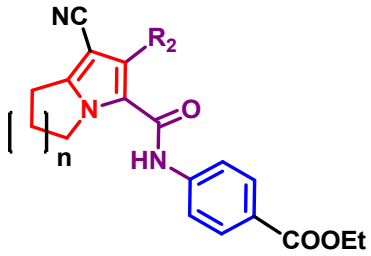

Comp. No	n	IC_{50} (µM)			
		MCF-7	A2780	HT29	MRC5
8a	1	0.07±0.01	0.45±0.10	0.70±0.12	2.00±1.01
8b	2	3.24±0.99	15.24±0.01	7.71±0.04	1.50±0.16
8c	3	2.87±0.13	4.25±1.21	12.87±0.57	3.21±0.43
9a	1	0.02±0.01	4.36±0.37	1.86±0.03	0.85±0.18
9b	2	18.52±1.42	23.35±2.67	3.57±0.48	22.45±3.65
10a	1	0.15±0.07	1.63±0.34	0.22±0.01	12.60±0.97
10b	2	0.37±0.05	14.65±1.36	1.83±0.02	13.95±0.35
11a	1	0.87±0.06	0.82±0.15	0.20±0.14	7.08±1.89
11b	2	0.82±0.11	0.06±0.01	0.17±0.01	3.38±0.29
Lapatinib	-	6.80±1.20	10.40±0.80	12.67±1.33	12.89±3.24

Results were presented as mean ± S.D. (n = 3), after 72 h treatment with test compounds or vehicle (control).

Compounds **8a-c** displayed potent cytotoxic activity against the three cancer cell lines with IC_{50} values in the range of 0.07-15.24 µM. Among these three derivatives, compound **8a** was the most active as cytotoxic agent. It exhibited IC_{50} values in submicromolar range against the three cancer cell lines. Among the three derivatives, compound **8b** which showed the highest selectivity toward COX-2 (**Table 4**), exhibited the lowest cytotoxic activity against both MCF-7 and A2780 cells.

The Schiff base **9a** displayed more than nine hundred times higher cytotoxic activity than compound **9b** against MCF-7 cells. Moreover, compound **9b** was the least active as a cytotoxic agent against both MCF-7 and A2780 cells. Moreover,

On the other hand, compounds **10a**,**b** showed higher cytotoxicity against both A2780 and HT29 cells compared to the corresponding Schiff bases **9a**,**b**. Compound **10a** exhibited higher cytotoxic activity against the three cancer cells compared to the indolizine analog **10b**. The two ibuprofen hybrids **11a,b** displayed IC_{50} values in submicromolar ranges against the three cancer cell lines. The

indolizine bearing derivative **11b** showed more than 10 times higher cytotoxicity than compound **11a** against A2780 cells. These results indicated that pyrrolizine bearing derivatives **8-10a** are more active as cytotoxic agents than their corresponding indolizine analogs **8-10b** against the three cancer cell lines.

2.2.6.2. Structure activity relationship (SAR)

Compound **8a** displayed high cytotoxic activity against the three cancer cell lines (IC_{50} = 0.07-0.70 μM). Expansion of the pyrrolidine ring in compound **8a** into piperidine was associated with decrease in both COX-2 inhibitory activity and cytotoxicity against the three cancer cell lines. However, expansion of piperidine ring in compound **8b** to azepine resulted in a decrease in COX-2 inhibitory activity with an improvement in cytotoxicity against MCF-7 and A2780 cells, **Tables 4** and **5**.

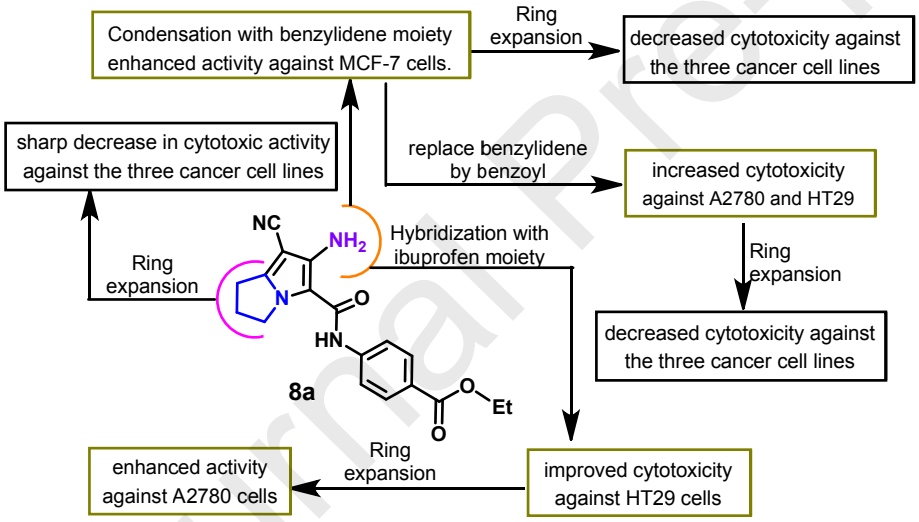

Fig. 6. SAR of cytotoxic activity of compounds **8-11**.

Cytotoxic activity against MCF-7 cells was improved, while COX-2 inhibitory activity was decreased on condensation of compound **8a** with benzaldehyde. On the other hand, expansion of the pyrrolizine ring in compound **9a** to piperidine was associated with increase in an COX-2 inhibitory activity and decrease in growth inhibitory activity against the three cancer cell lines, **Fig. 6**.

Moreover, benzoylation of compound **8a** improved cytotoxicity against HT29 cells, while MCF-7 and A2780 cells became less sensitive. This activity was decreased on expansion of pyrrolizine ring in compound **10a** to piperidine, **Fig. 6**.

Hybridization of compounds **8a**,**b** with ibuprofen moiety resulted in compounds that displayed IC_{50} values at the submicromolar ranges against the tested cell lines. Ring expansion to piperidine enhanced cytotoxic activity against A2780 cells, **Fig. 6**.

2.2.6.3. Cytotoxic selectivity

The ideal anticancer agent must have high cytotoxic selectivity toward tumor cells. To evaluate the cytotoxic selectivity of our new compounds **8-11**, their growth inhibitory activity was evaluated against a normal non-transformed human fibroblast cell line (MRC5). The study was performed using the MTT assay [35]. The results expressed in IC_{50} values were summarized in **Table 5**. Cytotoxic selectivity index (SI) was calculated for each of the new compounds by dividing the IC_{50} value of the test compound against normal non-cancer MRC5 cells by its IC_{50} value against cancer cells, **Fig. 7**.

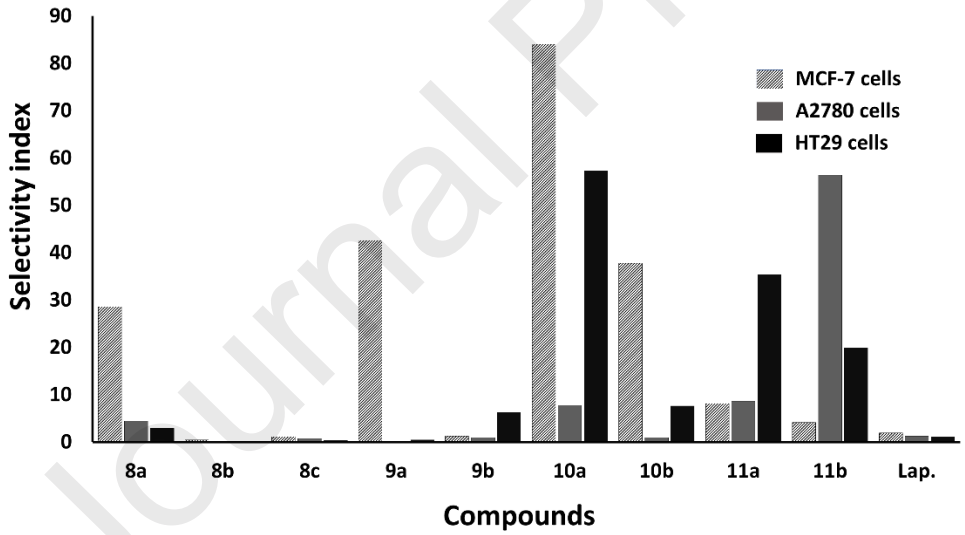

Fig. 7. Selectivity indices (IC_{50} value against MRC5 cell line/ IC_{50} value against cancer cell line) of compounds **8-11** toward MCF-7, A2780 and HT29 cancer cell lines.

Compound **8a** displayed SI in the range of 3-29 toward the three cancer cell lines, while the indolizine **8b** and pyrroloazepine **8c** were not selective. Compound **9a** was 43 times more selective for MCF-7 than the normal MCR5 cells, while compound **9b** was only 6 times more selective toward HT29 than MRC5 cells.

A remarkable increase in cytotoxic selectivity was observed for compounds **10a,b** compared to the parent compounds **8a,b**. They displayed SIs in the range of 1-84 toward the three cancer cell lines. The highest selectivity of the two compounds was observed toward MCF-7 cells.
Moreover, compounds **11a,b** were also more selective toward the three cancer cell lines than MCR5 cells. Compound **11a** displayed SI in the range of 8-35, while compound **11b** was 4-56 times more selective toward the three cancer cell lines. Compounds **10a**,**b** and **11a**,**b** exhibited higher selectivity toward the three cancer cell lines compared to lapatinib (SI = 1-2), **Fig. 7**.

2.2.7. Cell cycle analysis

MCF-7 cells were chosen for further explanations of the mechanistic actions of the new compounds as the highest selectivity observed was towards this cell line. For this, cell cycle analysis of MCF-7 cells treated with compound **9a** (24h) was performed using a Novocyte flow cytometer (Acea Biosciences, USA). Compound **9a** was selected for this study due to its high cytotoxic activity (IC_{50} = 0.02 µM) and cytotoxic selectively (SI = 43). Cell cycle analysis was performed according to our previous report [35]. The results were presented in **Table 6** and **Fig. 8**.

Table 6. Cell cycle analysis of MCF-7 cells treated with compound **9a** (24h).

Cell Cycle Stage/%	%			
	Control	**0.1 µM**	**0.5 µM**	**1 µM**
Sub G1	3.0±0.9	1.6±0.4	1.9±0.2	1.7±0.4
G1	49.6±0.6	57.6±1.2	60.1±1.5	56.6±1.4
S	28.5±1.6	16.8±0.3	15.8±1.6	18.0±1.7
G2/M	17.2±1.5	18.5±1.0	17.6±2.2	17.8±1.6

The distribution of different phases was analysed using the cell cycle algorithm of the NovoExpress software and expressed as percentage of total gated single events. Compared to the control, compound **9a** increased the percentage of cells in the G1 phase at 0.1 µM. This increase was also maintained at 0.5 and 1 µM and was mainly at the expense of cell accumulation in the S stage.

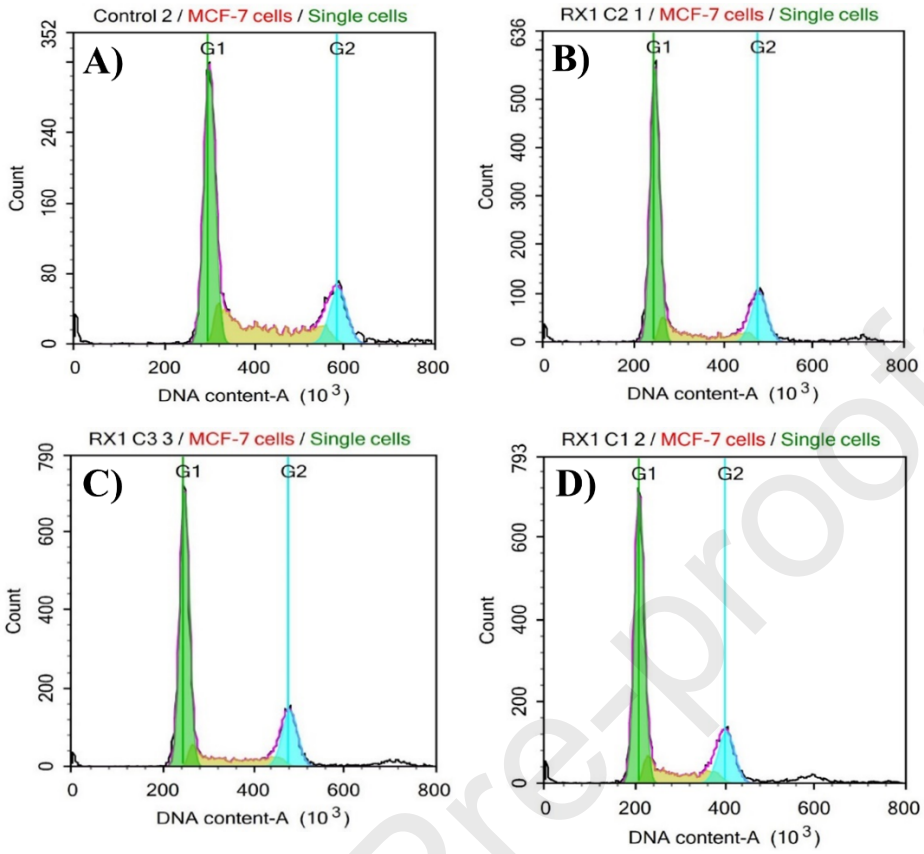

Fig. 8. Flow cytometry histograms showing the effect of compound **9a** on cell cycle distribution of MCF-7 cells after 24h treatment. X-axis: DNA content of 20,000 events, y axis: cell number. a): 0μM; b): 0.1μM; c): 0.5μM; d): 1 μM. (n = 3). Experiment was repeated 3x.

2.2.8. Annexin V-FITC/PI apoptosis assay

The anticancer activity of several NSAIDs was mediated by induction of apoptosis in different types of cancer cell lines [9-11]. In addition, the anticancer activity of licofelone **1** and ketorolac **2** were mediated by induction of apoptosis in colon, prostate and osteosarcoma cancer cell lines [17,18,36]. Accordingly, the ability of compound **9a** to induce apoptosis in MCF-7 cells was investigated in this work. Annexin V fluorescein isothiocyanate (FITC)/ propidium iodide (PI) apoptosis assay was used in this study according to our previous reports [30,34]. The results were presented in **Fig. 9**. Compound **9a** induced a dose-dependent increase in the apoptotic events of MCF-7 cells compared to control.

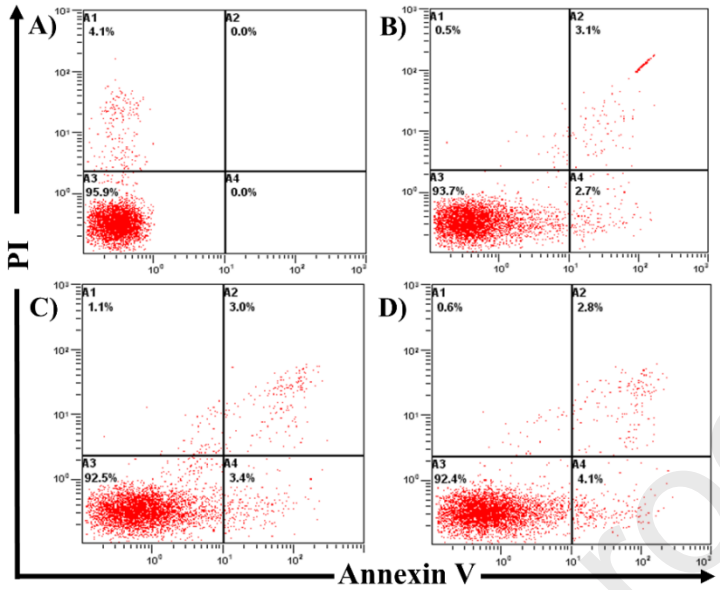

Fig. 9. Evaluation of apoptosis-inducing activity of compound **9a** in MCF-7 cells using annexin V FITC/PI staining assay, cells were treated with compound **9a** for 24h at: a) 0 µM, b) 0.1 µM, c) 0.5 µM, d) 1 µM (*n* = 3). x-axis: annexin V/FITC, y-axis: PI. C1: necrosis, PI+/annexin V-); C2: (late apoptosis, PI+/ annexin V+); C3: (living cells, PI-/annexin V-); C4: (early apoptosis, PI-/annexin V+).

The effect of compound **9a** on apoptotic events in MCF-7cells was determined based on the results of annexin V-FITC/PI assay. Compound **9a** induced 5.8% increase in apoptotic events (late plus early apoptosis) in MCF-7 cells at 0.1 µM, compared to the control (0%). A slight increase in apoptotic evets to 6.4% and 6.9% was observed at 0.5 and 1 µM, respectively. These results indicated that the compound **9a** include apoptosis at a dose of ≤ 0.1 µM. Only, slight necrosis (0.5-1.1%) was observed in the MCF-7 cells treated with compound **9a**, compared to 4.1% for control, **Fig. 10.**

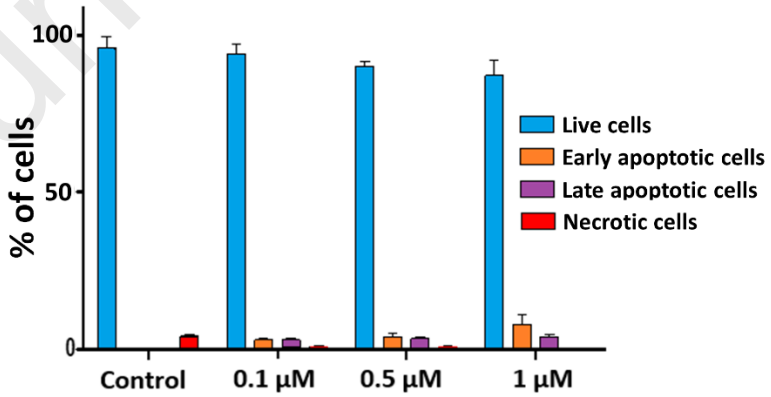

Fig. 10. Bar graph showing the effect of treatment with compound **9a** (24h) on MCF-7 cells stained with annexin V-FITC (x-axis), and PI. Data shown are % mean ± SD (n=3). Experiment was repeated 3x.

2.3. Computational studies

2.3.1. Molecular docking studies

COXs inhibition is the main mechanism of action of NSAIDs [37]. Compounds **8-10** exhibited COX-1/2 inhibitory activity, **Table 4**. Based on these results, a comparative molecular docking study was performed to evaluate binding affinities/modes of the new compounds **8-11** into the active site the two enzymes. The study was performed using AutoDock 4.2 [38]. Crystal structure of both COX-1 [39] and COX-2 [40] were obtained from protein data bank (http://www.rcsb.org/pdb/home/home.do).

Preparation of ligand, protein file and grid/docking parameters were done according to our previous reports [41,42]. Visualization of binding interactions of the new compounds with different amino acids in the active sites of COXs was generated by LigPlot^{+} [43] and Discovery Studio Visualizer [44]. The binding free energies and inhibition constants of the new compounds were also evaluated.

2.3.1.1. Docking study into COX-1 enzyme

The native ligand (ibuprofen) of COX-1 (pdb: 1EQG) was initially re-docked into the active site of the enzyme to validate the docking protocol [41,42]. The results revealed superimposition of redocked ibuprofen above the co-crystallized ligand with RMSD of 0.87 Å. The new compounds were docked into COX-1 and docking results were compared with that of compound **3**, **Table 7**.

The results of the docking study revealed the ability of compounds **8-11** to form 1-4 conventional hydrogen bonds with ARG83, ARG120, VAL349, TYR355 and SER530 in the active site of COX-1. The new compounds exhibited binding free energy (ΔG_b) in the range of -8.53 to -10.15 kcal/mol, compared to -8.43 kcal/mol for ibuprofen and -9.50 kcal/mol for compound **3**. The new compounds also displayed inhibition constants (K_i) in the range of 36.43-561.1 nM compared to 664 nM for ibuprofen. The results suggested that all of the new compounds have higher inhibitory activity against COX-1 than ibuprofen, **Table 7**.

Compound **8c** displayed the highest binding free energy to COX-1 with (ΔG_b = -10.15 kcal/mol, K_i = 36.43 nM), while compound **8b** exhibited the lowest affinity. Moreover, compounds **9a**,**b** and **10a**,**b** displayed higher affinity to COX-1 than their parent compounds **8a**,**b**. On the other hand, compound **11a** showed higher affinity to COX-1 than parent **8a**, while the indolizine analog **11b** exhibited comparable affinity to the parent **8b**.

Table 7. Results of the docking of compounds **8-11** into ovine COX-1 (pdb: 1EQG) [39] in comparison to compound **3** and the co-crystallized ligand (ibuprofen).

Comp. No	ΔG_b [a]	K_i [b]	HBs [c]	Atoms in H-bonding		Length [d]
				In ligand	In COX-1	(Å)
8a	-9.32	148.2 nM	3	COOEt	NH_2 of ARG120	2.00
				COOEt	NH_2 of ARG120	2.04
				NH_2	NH of ARG120	2.14
8b	-8.53	561.1 nM	3	COOEt	NH_2 of ARG120	1.96
				COOEt	OH of TYR355	2.14
				NH_2	C=O of VAL349	3.08
8c	-10.15	36.43 nM	4	PhNHCO	OH of SER530	1.70
				COOEt	OH of TYR355	1.74
				COOEt	NH_2 of ARG120	1.85
				NH_2	C=O of VAL349	2.16
9a	-9.03	241.87 nM	2	Ph-NHCO	OH of TYR355	2.23
				Ph-NHCO	NH_2 of ARG120	2.36
9b	-8.74	393.91 nM	2	Ph-NHCO	NH_2 of ARG120	2.00
				Ph-NHCO	OH of TYR355	2.22
10a	-9.52	104.59 nM	1	CN	NH_2 of ARG83	1.94
10b	-9.99	47.20 nM	1	CN	NH_2 of ARG83	1.97
11a	-9.95	50.89 nM	3	Ph-NHCO	NH_2 of ARG120	1.80
				Ph-NHCO	OH of TYR355	1.91
				CN	OH of SER530	2.56
11b	-8.56	535.29 nM	2	CN	NH of ARG83	2.12
				CN	NH_2 of ARG83	2.84
3	-9.50	109.54 nM	4	NH_2	C=O of MET522	2.22
				OH	OH of TYR355	1.99
				OH	NH_2 of ARG120	1.80
				COOEt	NH_2 of ARG120	1.89
Ibu.	-8.43	664 nM	3	C=O	NH of ARG120	1.71
				COOH	NH_2 of ARG120	1.79
				COOH	OH of TYR355	1.83

[a] Binding free energy; [b] inhibition constant; [c] number of hydrogen bonds; [d] length in angstrom (Å).

2.3.1.2. Docking study into COX-2 enzyme

To validate the docking procedures into COX-2 (pdb: 1CX2), the native ligand (SC-558) was re-docked into the active site of the enzyme. The result revealed superimposition of SC-558 above the native SC-558 with RMSD of 1.56 Å. SC-588 displayed inhibition constant (Ki) of 12.52 nM. This value was slightly higher than its IC_{50} value (9.3 nM) against COX-2 [40].

The new compounds **8-11** were docked into the active site of COX-2 and the results were summarized in **Table 8**. The new compounds exhibited binding free energy in the range of -9.00-12.39 kcal/mol, compared to -10.78 kcal/mol for SC-558. They displayed also inhibition constant in the range of 0.83-253.45 nM. The results revealed the formation of 1-3 conventional hydrogen bonds with amino acids in the active site of COX-2. Compound **9b** displayed the highest affinity for COX-2 with binding free energy of ΔG_b of -12.39 and inhibition constant of 0.830 nM. Moreover, compound **10b** also displayed high binding free energy to COX-2 with ΔG_b of -12.26 kcal/mol and inhibition constant of 1.03 nM. Due to their high affinities to COX-2, compounds **9a**,**b** and **10a**,**b** exhibited higher selectivity for COX-2 than their parent compounds **8a**,**b**.

Table 8. Results of the docking of compounds **8-11** into COX-2 (pdb: 1CX2) [40] in comparison to compound **3** and the native co-crystallized SC-558.

Comp. No	ΔG_b [a]	K_i	HBs [c]	Atoms in H-bonding		Length [c] (Å)
				In ligand	In COX-2	
8a	-10.08	40.98 nM	2	COOEt	NH_2 of ARG513	2.86
				NH_2	C=O of VAL523	2.49
8b	-10.05	43.3 nM	2	NH_2	C=O of VAL523	1.95
				COOEt	NH_2 of ARG513	2.01
8c	-10.29	28.87 nM	3	NH_2	C=O of VAL523	2.08
				COOEt	NH_2 of ARG513	2.09
				NH_2	C=O of VAL523	2.14
9a	-11.79	2.26 nM	3	COOEt	NH of PHE518	2.79
				COOEt	NH_2 of GLN192	2.97
				COOEt	NH of ILE517	2.99
9b	-12.39	0.830 nM	2	COOEt	NH of ILE517	2.56
				COOEt	NH^1 of HIS90	2.97
10a	-11.20	6.15 nM	3	PhNHCO	OH of TYR355	2.29
				PhNHCO	NH_2 of ARG120	2.57
				CN	OH of SER530	2.93
10b	-12.26	1.03 nM	3	COOEt	NH of PHE518	2.35
				PhNHCO	OH of TYR355	2.78
				COOEt	NH of ILE517	2.86
11a	-10.43	22.54 nM	1	PhNHCO	NH_2 of ARG120	2.45
11b	-9.00	253.45 nM	1	CN	NH_2 of ARG120	2.68
3	-9.01	247.26 nM	4	COOEt	NH_2 of ARG513	1.96
				COOH	C=O of SER353	1.98
				NH_2	C=O of VAL523	2.21
				NH_2	C=O of VAL523	2.25
Sc-588	-10.78	12.52 nM	5	SO_2	NH of HIS90	2.88
				NH_2	CO of LEU352	2.08
				NH_2	CO of GLN192	1.97

CF_3	NH of ARG120	3.22
CF_3	NH of ARG120	3.58

[a] Binding free energy; [b] inhibition constant; [c] number of hydrogen bonds; [d] length in angstrom (Å).

Compounds **8a-c** displayed higher affinity toward COX-2, where compound 8a exhibited the highest affinity toward COX-2. These results was in agreement the in vitro COX-1/2 inhibitory activities. Moreover, compounds **9a**,**b** and **10a**,**b** displayed very high affinity to COX-2 in docking results. This was also matched with the results of *in vitro* COXs inhibitory activity. Compound **9b 10b** showed higher COX-2 inhibitory activity than their corresponding pyrrolizine derivative **9a** and **10a**. These results were also in concordance with the results of COXs inhibition assay. The correlation coefficient was calculated between selective indices (SIs) of the new compounds to COX-2 (**Table 4**) and the calculated selectivity obtained by dividing the K_i values of the new compounds against COX-1 by K_i values against COX-2 enzyme (Table S3, supplementary data). The results revealed a correlation coefficient of 0.902 indicating strong correlation between docking results and the *in vitro* results of COX-1/2 inhibition.

Although compound **3** has a free carboxylic acid group which can form multiple hydrogen bond with COXs, but the ethyl ester **8a** displayed higher affinity to COX-2 (ΔG_b = -10.08 kcal/mol) than compound **3** (ΔG_b = -9.01). To understand the reasons behind this difference 2D LigPlot view was generated for compounds **3** and **8a** in the active site of COX-2, **Fig. 11**. The plot showed different types of hydrogen bonding and hydrophobic interactions between the two compounds and COX-2. The red circles and ellipses indicate protein residues which form similar types of interactions with the two ligands. Compound **8a** formed only two conventional hydrogen bonds with COX-2 compared to four hydrogen bonds for compound **3**. However compound **8a** displayed larger number of hydrophobic interactions with COX-2 than compound **3**, **Fig. 11**. These hydrophobic interactions could justify the higher affinity of compound **8a** toward COX-2 compared to compound **3**.

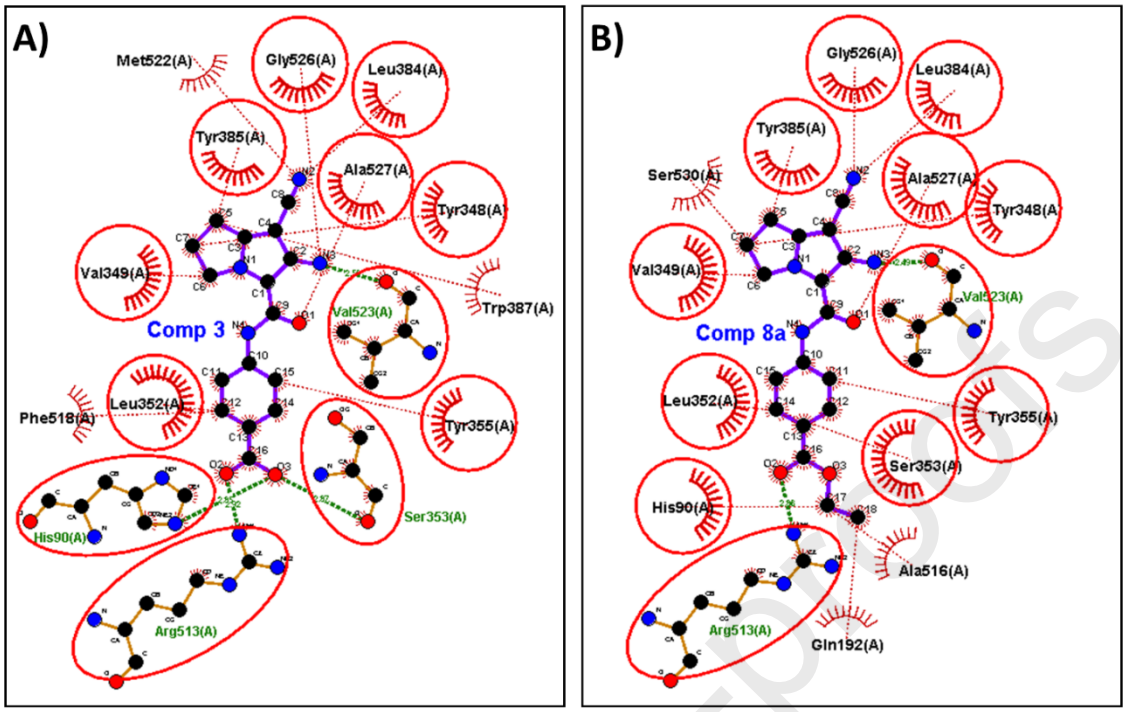

Fig. 11. LigPlot view of showing different types of binding interactions between compounds **3**/**8a** and amino acids in the active site of COX-2 (pdb: 1CX2): A) compound **3**; B) compound **8a**. Ligand bonds shown in purple. The red circles and ellipses in each plot indicate protein residues that are in equivalent 3D positions and form similar types of interactions with the two ligands, hydrophobic interactions shown in brick red dotted lines and hydrogen bonding interactions shown in olive green dotted lines. Hydrogen atoms were omitted for clarity.

The three indolizine bearing derivatives **8**-**10b** displayed higher inhibitory activity and selectivity (**Table 4**) against COX-2 than their pyrrolizine analogs **8**-**10a**. Compound **8b** displayed three conventional hydrogen bonds with ARG120, VAL349 and TYR355 in COX-1, with bond length in the range of 1.96-3.08 Å and one carbon hydrogen bond with MET522, **Table 7**. Different types of hydrophobic interactions were also observed between the indolizine nucleus, phenyl ring, and ethyl group in compound **8b** with hydrophobic residues in COX-1, **Fig. 12**. On the other hand, compound **8b** displayed two conventional hydrogen bonds with COX-2. These bonds were formed with VAL523 and ARG513 with bond length of 1.95 and 2.01 Å, respectively, **Table 8**. Moreover, two carbon hydrogen bonds were observed with GLA192 and ARG513 amino acids. It showed several hydrophobic interactions with COX-2, **Fig. 12**. The high affinity of compound **8b** toward COX-2 could be attributed to the extra carbon hydrogen bonds and stronger hydrophobic interactions observed with COX-2 compared to COX-1.

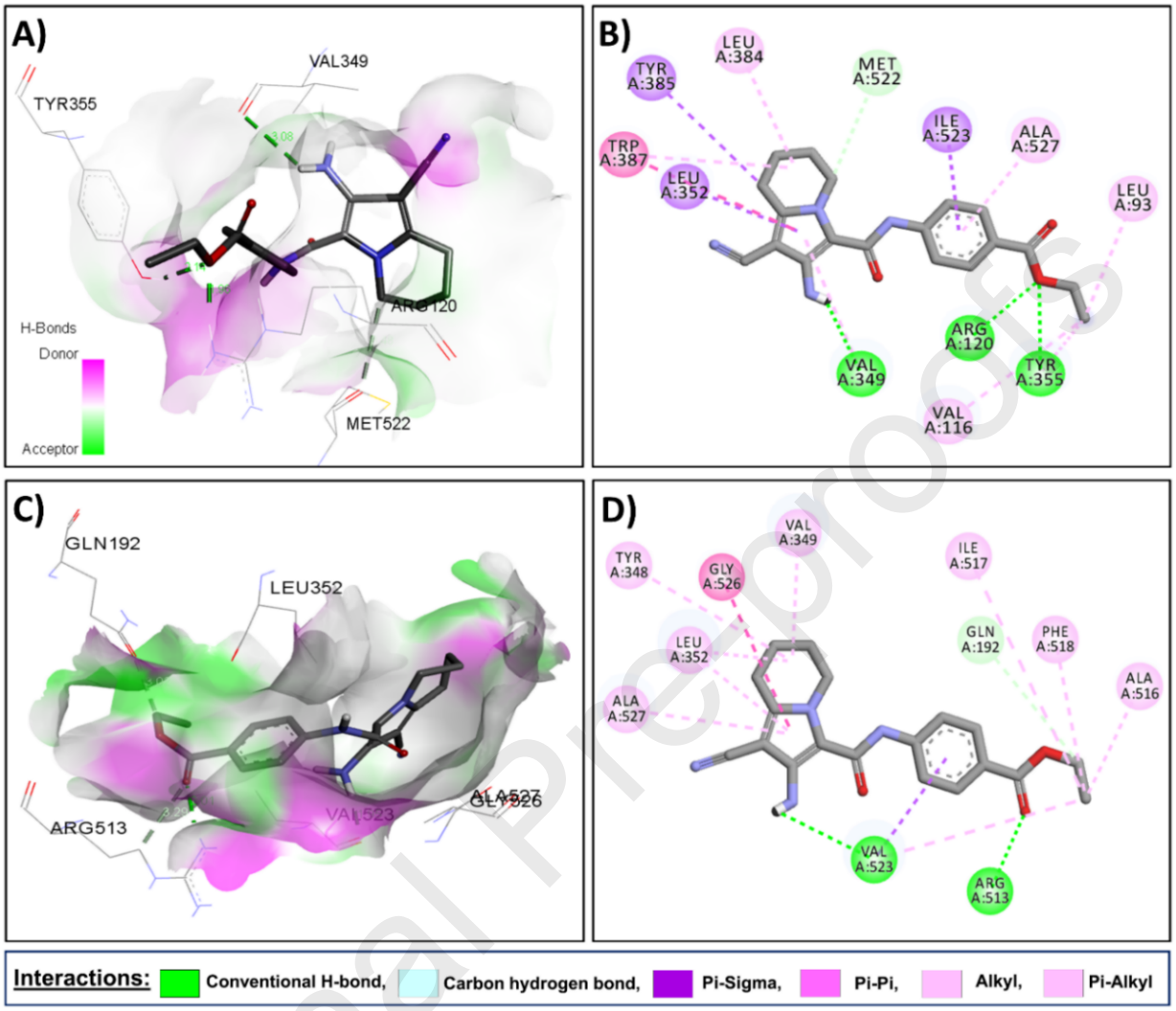

Fig. 12. Binding modes/interactions of compound **8b** (shown as stick, colored by element) into the active site of COXs: A) 3D binding mode into COX-1 (pdb code: 1EQG); B) 2D binding mode into COX-1; C) 3D binding mode into COX-2 (pdb: 1CX2); D) 2D binding mode into COX-2; receptor surface shown as H-bond donor (red) and acceptor (green); hydrogen atoms were omitted for clarity.

Compound **9b** displayed binding free energy of -8.74 and -12.39 kcal/ mol for COX-1 and COX-2, respectively. It exhibited two conventional hydrogen bonds with both COX-1 and COX-2. Other binding interaction of carbon hydrogen, pi-cation/anion and pi-sulfur types were also observed between compound **9b** and COX-1/2. However, compound **9b** displayed larger number of hydrophobic interaction (15 interactions) with COX-2 than COX-1 (7 interactions). These interactions could account for the higher affinity of compound **9b** to COX-2 than COX-1, **Fig. 13**.

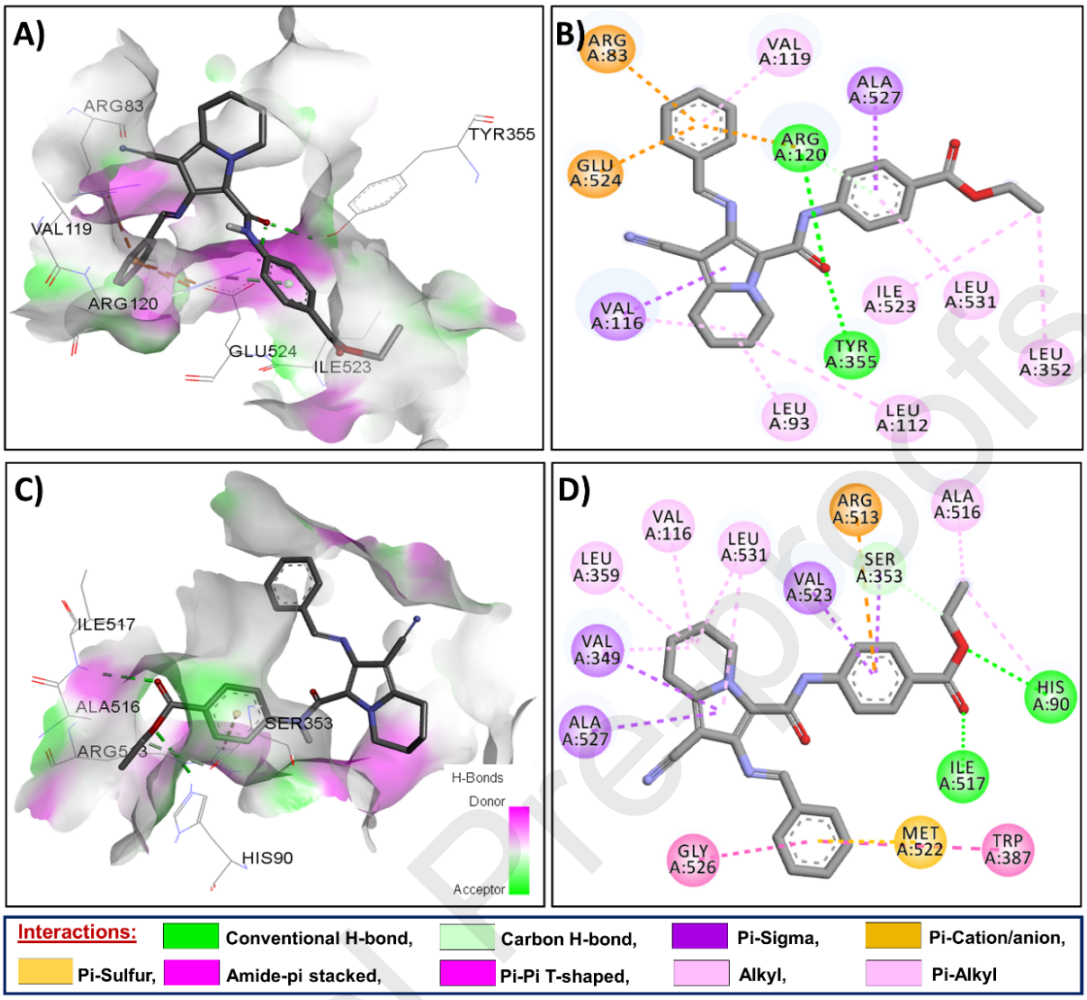

Fig. 13. Binding modes/interactions of compound **9b** (shown as stick, colored by element) into the active site of COXs: A) 3D binding mode into COX-1 (pdb code: 1EQG); B) 2D binding mode into COX-1; C) 3D binding mode into COX-2 (pdb: 1CX2); D) 2D binding mode into COX-2; receptor surface shown as H-bond donor (red) and acceptor (green); hydrogen atoms were omitted for clarity.

Compound **10b** also displayed higher affinity for COX-2 (ΔG = -8.53) than COX-1 (ΔG = -12.26). It formed one conventional hydrogen bond with ARG83 in COX-1 compared to three conventional hydrogen bonds with TYR355, ILE517 and PHE518 in COX-2. Compound **10b** exhibited one carbon hydrogen bond and one pi-sulfur interaction with COX-2 while no interaction of these types was observed with COX-1. Moreover, compound **10b** showed larger number of pi-sigma and hydrophobic interactions with COX-2 than with COX-1. As in results, **Fig. 14**.

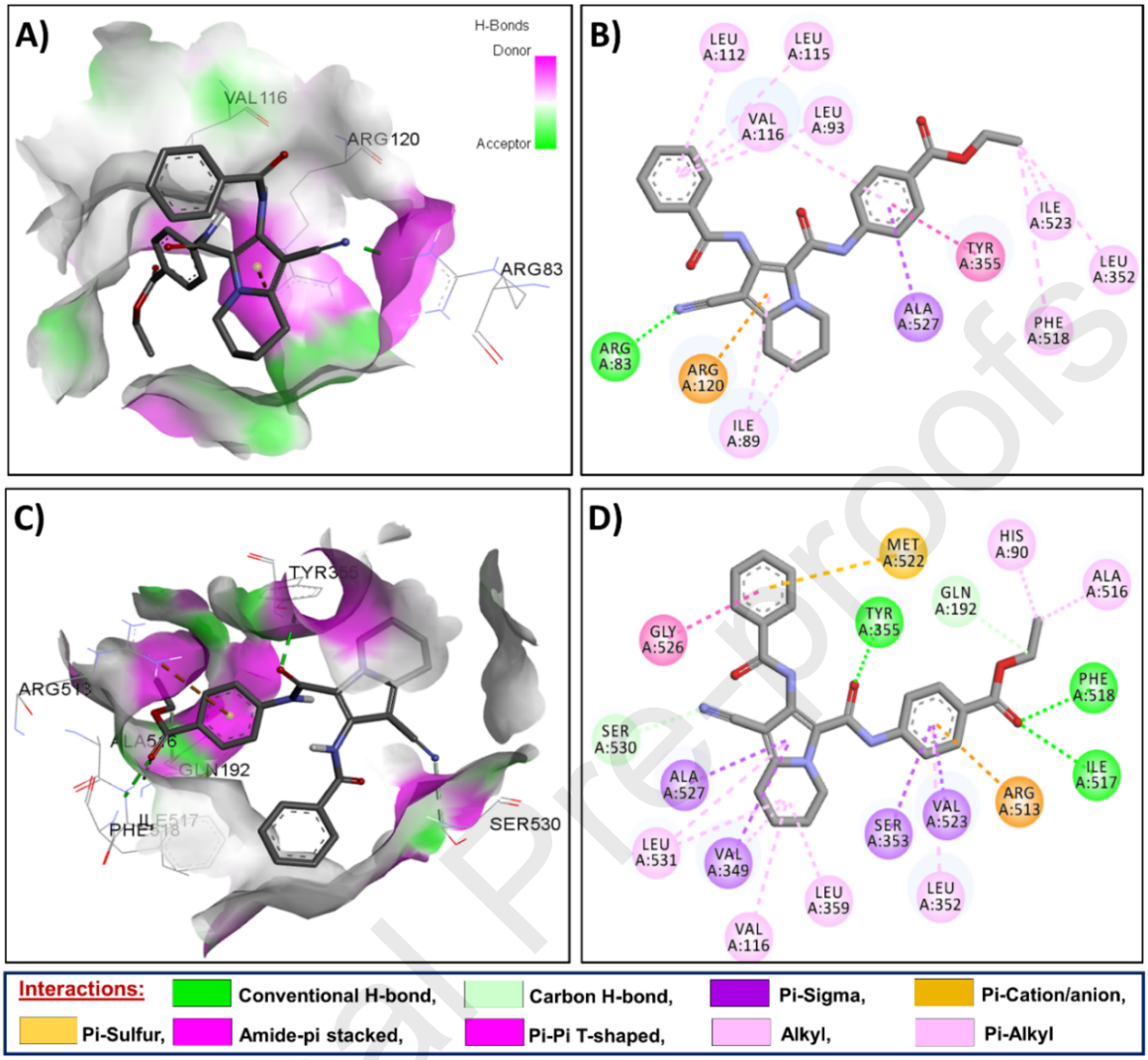

Fig. 14. Binding modes/interactions of compound **10b** (shown as stick, colored by element) into the active site of COXs: A) 3D binding mode into COX-1 (pdb code: 1EQG); B) 2D binding mode into COX-1; C) 3D binding mode into COX-2 (pdb: 1CX2); D) 2D binding mode into COX-2; receptor surface shown as H-bond donor (red) and acceptor (green); hydrogen atoms were omitted for clarity.

2.3.2. Drug-likeness and ADME studies

Large numbers of anticancer agents are reported every year with potent antiproliferative activity. However, only a very few numbers of these compounds succeeded to pass to the early clinical investigation phase [45,46]. One of the reasons behind this failure is the pharmacokinetic problems. In this study, drug-likeness and ADME parameters of the new compounds **8-11** were investigated according to our previous report [30].

SwissADME developed by the Molecular Modeling Group of the Swiss Institute of Bioinformatics was used to predict physicochemical properties of the new compounds [47]. Drug-likeness parameters of the tested compounds **8-11** were evaluated according to Lipinski's rule [48] in comparison to compounds **1** and **2**. The results were summarized in **Table 9**. The results revealed no violation of Lipinski's rule for compounds **8-10**. In addition, these compounds showed no violation of Ghose, Veber, Egan and Muegge rules. On the other hand, compounds **11a**,**b** and **12** showed only one violation of Lipinski's rule.

Table 9. Molecular properties related to drug-likeness of compounds **1-3** and **8-12**.

Comp. No	Physicochemical properties							Lipinski's rule	%Abs [a]	BS	DLS [b]
	MW	MV[a]	TPSA	MlogP	RBs	H_A	H_D				
8a	338.36	349.99	110.14	0.93	6	4	2	Yes	71.00	0.55	**0.89**
8b	352.39	367.00	110.14	1.16	6	4	2	Yes	71.00	0.55	**1.06**
8c	366.41	392.07	110.14	1.39	6	4	2	Yes	71.00	0.55	**0.96**
9a	426.47	445.86	96.48	2.17	8	5	1	Yes	75.71	0.55	0.67
9b	440.49	462.87	96.48	2.38	8	5	1	Yes	75.71	0.55	0.85
10a	442.47	457.52	113.22	1.79	9	5	2	Yes	69.94	0.55	0.70
10b	456.49	474.53	113.22	2.00	9	5	2	Yes	69.94	0.55	0.89
11a	526.63	561.58	113.22	2.97	12	5	2	Yes [c]	69.94	0.55	**1.41**
11b	540.65	578.59	113.22	3.16	12	5	2	Yes [c]	69.94	0.55	**1.56**
12	730.73	763.77	226.44	4.76	17	10	4	Yes [d]	17.08	0.17	0.6
1	379.88	383.88	42.23	4.26	4	2	1	Yes [e]	94.43	0.56	1.06
2	255.27	254.26	59.30	1.24	3	3	1	Yes	88.54	0.56	0.52
3	310.31	309.51	121.14	0.45	4	4	3	Yes	67.21	0.56	1.02

[a] %Abs = 109 – (0.345 x TPSA); MV, molecular volume (A^3); [b] DLS, drug-likeness score; [c] one violation, molecular (weight >500); [d] two violations (MW >500, RBs >10); [e] one violation (MlogP > 4.15); MW and DLS were calculated using Molsoft (http://molsoft.com/mprop/)

The molecular weights (MW) of compounds **8-10** were in the range of 338-456 (< 500) and their calculated log P (MlogP) values were in the range 0.93-3.16 (<5). Based on these values, compounds **8-10** are expected to be more lipophilic than compound **3**, but less lipophilic than licofelone **1**. They have 6-8 rotatable bonds (RBs), 1/2 hydrogen bond donors ($H_D \leq 5$) and 4/5

hydrogen bond acceptors ($H_A \leq 10$). Accordingly, compounds **8-10** were expected to be drug-like and could have good oral bioavailability, **Table 9**.

Except for compound **12**, all the new compounds exhibited bioavailability score (BS) of 0.55, compared to 0.56 for licofelone **1** and ketorolac **2**. They displayed topological polar surface area (TPSA) in the range of 96.48-113.32 A^2 compared to 42.23 and 59.30 A^2 for licofelone and ketorolac, respectively.

Drug-likeness score (DLS) of the new compounds was calculated using Molsoft developed by Molsoft LLC (http://molsoft.com/mprop/). Compound **8-11** displayed drug-likeness scores in the range of 0.67-1.56 compared to 1.06 and 0.52 for licofelone **1** and ketorolac **2**, respectively. Among these derivatives, compounds **8b** and **11a**,**b** exhibited DLS in the range of 1.06-1.56, which was higher than ketorolac **2**. Compound **12** with the highest molecular weight (730.73) exhibited also the highest calculated log P (4.76) which could account for the poor solubility of compound **12** in organic solvents. Compound **12** displayed the lowest DLS (0.6).

GIT absorption percent (**%**Abs) was also calculated according to the method reported by Zhao *et al*. [49]. Except for compound **12**, all the new compounds displayed absorption percent (**%**Abs) in the range of 69.94-75.71%, compared to 88.54% for ketorolac **2**, **Table 9**

3. Conclusion

Two new series of ethyl benzoate bearing pyrrolizine and indolizine moieties were designed and synthesized. Chemical structure of the new compounds was confirmed by spectral and elemental analyses. The new compounds displayed 27.19-46.32% anti-inflammatory activity (4h post-carrageenan injection), compared to 53.78% for ibuprofen. Moreover, compounds **9a**, **10b** and **11b** displayed analgesic activity nearly equal to or slightly higher than that of ibuprofen. The acute ulcerogenicity studies revealed better GIT safety profile than ibuprofen. Moreover, histopathological studies revealed only few changes in histological features of gastric mucosa/submucosa. Mechanistic study revealed COX-1/2 inhibitory activity with preferential inhibition of COX-2. Among the tested derivatives, compound **9b** was the most selective COX-2 inhibitor (SI = 27.52). Evaluation of cytotoxicity of the new compounds using MTT assay revealed potent to moderate activity against three human (MCF-7, A2780 and HT29) cancer cell lines with IC_{50} values in the range of 0.02-23.35 μM. Among these derivatives, compound **9a** displayed the highest cytotoxic activity against MCF-7 (IC_{50} = 0.02 μM) cell line, while compound **11b** was the most active against both A2780 and HT29 cells. Compounds **10a**,**b** and **11a**,**b** exhibited cytotoxic selectivity index in the range of 1-84 against the three cancer cell lines. Cell cycle analysis and annexin V-FITC/PI assay revealed the ability of compound **9a** to induce G1 cell cycle arrest and apoptosis in MCF-7 cells. The results of the docking study revealed higher affinity for the new compounds to COX-2 than COX-1. These results were in concordance with the results of COX-1/2 inhibitory assay. The new compounds interacted mainly by hydrophobic interactions with amino acid in the active site of COX-1/2. The new compounds displayed also drug-likeness score in the range of 0.67-1.56 compared to 1.06 for licofelone. These results suggested that the new compounds reported in this work could be promising agents in future research as anti-inflammatory and anticancer agents.

4. Experimental protocol

4.1. Chemistry

Chemical reagents and solvents were obtained from commercial sources. Solvents are dried by standard methods when necessary. The purity of the new compounds was checked with TLC. Melting points (m.p.) are uncorrected and were determined by IA 9100MK-Digital melting point apparatus (Cole-Parmer, USA). Infrared spectra (IR) were recorded using BRUKER TENSOR 37 spectrophotometer (Bruker, Germany) from KBr discs. The proton magnetic spectra were recorded on BRUKER AVANCE III at 500 MHz (Bruker, Germany) in the specified solvent and *J* constants were given in Hz. The ^{13}C NMR and DEPT C^{135} (Distortionless enhancement by polarization transfer) spectra of the new compounds in the specified solvent were done on BRUKER AVANCE III (Bruker, Germany) at 125 MHz. Mass spectra were recorded on Agilent 6420 LC/MS 1260 infinity system with triple quad detector at the faculty of pharmacy, Minia University. All mass spectra were recorded in EI mode.

4.1.1. General procedure (A) for preparation of compounds (5a-c)

Compounds **5a-c** were prepared according to the previous report [26-28]. Briefly, dimethyl sulfate (7.4g, 58.8 mmol) was added to a solution of the lactam (2-pyrrolidinone, piperidin-2-one or azepan-2-one) (58.8 mmol) in dry benzene (20 ml). The reaction mixture was stirred under reflux for 3 hours then allowed to cool to room temperature. The solution was rendered alkaline with sodium hydroxide (3 ml, 600 g/L). The organic phase was separated, dried over anhydrous sodium sulfate and filtered. Malononitrile (2.5g, 38.2 mmol.) was added with stirring to the dried benzene layer. The reaction mixture was set aside to evaporate whereby white crystals were formed.

4.1.1.1. 2-Pyrrolidin-2-ylidene-malononitrile (5a)

Compound **5a** was prepared from 2-pyrrolidinone using the general procedure A. Compound **5a** was obtained as white crystals product, m.p. 159-61ºC (reported 158-9ºC), yield 75%.

4.1.1.2. 2-(Piperidin-2-ylidene)malononitrile (5b)

Compound **5b** was prepared from piperidin-2-one using the general procedure A. Compound **5b** was obtained as white crystals product, yield 71%.

4.1.1.3. 2-(Azepan-2-ylidene)malononitrile (5c)

Compound **5c** was prepared from azepan-2-one using the general procedure A. Compound **5c** was obtained as white crystals product, yield 65%.

4.1.2. Preparation of compounds (7)

To a solution of benzocaine **6** (54 mmol) in glacial acetic acid (20 ml), chloroacetyl chloride (9.1g, 81 mmol) and saturated aqueous solution of sodium acetate (10 ml) was added dropwise according to the previous report [29]. A heavy precipitate was formed shortly after addition. Stirring was continued for additional one hour. The separated product was filtered, washed with water and recrystallized from aqueous ethanol, yield 78%.

4.1.3. General procedure (B) for preparation of compounds (8a-c)

A mixture of ethyl benzoate **7** (1.81 g, 7.5 mmol), compound **5a-c** (7.5 mmol), and anhydrous potassium carbonate (1.04 g, 7.5 mmol) in dry acetone (50 mL) was stirred under reflux for 24 hours according to the previous report [29]. The reaction mixture was filtered while hot, concentrated and left to cool. The solid product separated was collected, dried and recrystallized from ethanol-acetone mixture.

4.1.3.1. Ethyl 4-(6-amino-7-cyano-2,3-dihydro-1*H*-pyrrolizine-5-carboxamido)benzoate (8a)

The title compound was prepared from the reaction of ethyl benzoate **7** (1.81 g, 7.5 mmol) with compound **5a** (1 g, 7.5 mmol) according to the general procedure B. Compound **8a** was reported by our research lab [29]. Compound **8a** was obtained as yellowish white solid product, m.p. 228-30 °C, yield 62%. IRυ_{max}/cm^{-1} 3448, 3340, 3300 (NHs), 3038 (C-H aromatic), 2927 (C-H aliphatic), 2210 (CN), 1699, 1638 (C=O). ^{1}H-NMR ($CDCl_3$, 500 MHz, δ ppm): δ 1.42 (t, 3H, J = 7.0 Hz, CH_3), 2.56 (m, 2H, pyrrolizine CH_2-2), 3.02 (t, 2H, J = 7.5 Hz, pyrrolizine CH_2-1), 3.60 (s, 2H, NH_2), 4.37-4.44 (m, 4H, ester OCH_2 + pyrrolizine CH_2-3), 7.68 (d, 2H, J = 10 Hz, aromatic CH-3+CH-5), 8.05 (d, 2H, J = 10 Hz, aromatic CH-2+CH-6), 9.84 (s, H, NH). ^{13}C-NMR ($CDCl_3$, 125 MHz, δ ppm): δ 14.37 (CH_3), 24.79 (pyrrolizine CH_2-2), 25.43 (pyrrolizine CH_2-1), 49.75 (pyrrolizine CH_2-3), 60.81 (OCH_2), 83.58 (pyrrolizine C-7), 114.25 (CN), 114.59 (aromatic C-1), 118.71 (2C, aromatic CH-3+CH-5), 125.56 (pyrrolizine C-5), 130.85 (2C,

aromatic CH-2+CH-6), 137.66 (pyrrolizine C-7a), 142.35 (aromatic C-4), 145.58 (pyrrolizine C-6), 158.70 (CONH), 166.19 (COOEt). DEPT C^{135} ($CDCl_3$, 125 MHz, δ ppm): δ 14.37 (CH_3), 24.79 (CH_2-1), 25.44 (CH_2-2), 49.76 (CH_2-3), 60.81 (OCH_3), 118.71 (aromatic CH-2 + CH-6), 130.85 (aromatic CH-3 + CH-5). MS (EI): m/z (%) 339 (M^++1, 3), 338 (M^+, 16), 324 (2), 293 (2), 265 (1), 237 (1), 174 (100), 146 (41), 120 (21), 105 (3), 92 (27), 77 (2).

4.1.3.2. Ethyl 4-(2-amino-1-cyano-5,6,7,8-tetrahydroindolizine-3-carboxamido)benzoate (8b)

The title compound was prepared from the reaction of ethyl 4-(2-chloroacetamido)benzoate **7** (1.81 g, 7.5 mmol) with compound **5b** (1.1 g, 7.5 mmol) according to the general procedure B. Compound **8b** was obtained as white solid product, m.p. 239-41 °C, yield 54%. IRυ_{max}/cm^{-1} 3349, 3282 (NHs), 3068, 3003 (C-H aromatic), 2967, 2932, 2908 (C-H aliphatic), 2211 (CN), 1699, 1672 (C=Os), 1595, 1540 (C=C, C=N), 1427, 1415, 1279 (C-C, C-N). ^{1}H-NMR (DMSO-d_6, 500 MHz, δ ppm): δ 1.32 (t, 3H, J = 7.1 Hz, CH_3), 1.76 (m, 2H, indolizine CH_2-7), 1.87 (m, 2H, indolizine CH_2-6), 2.77 (t, 2H, J = 6.2 Hz, indolizine CH_2-8), 4.10 (t, 2H, J = 5.9 Hz, indolizine CH_2-5), 4.29 (q, 2H, J = 7.1 Hz, OCH_2), 5.35 (s, 2H, NH_2), 7.71 (d, 2H, J = 8.9 Hz, aromatic CH-3, CH-5), 7.90 (d, 2H, J = 9.0 Hz, aromatic CH-2, CH-6), 9.82 (s, H, CONH). ^{13}C-NMR (DMSO, 125 MHz, δ ppm): δ 14.71 (CH_3), 19.00 (indolizine CH_2-7), 22.75 (indolizine CH_2-8), 22.82 (indolizine CH_2-6), 45.84 (indolizine CH_2-5), 60.84 (OCH_2), 82.02 (indolizine C-1), 110.87 (CN), 119.41 (2C, aromatic CH-3+CH-5), 124.10 (aromatic C-1), 124.97 (indolizine C-3), 130.49(2C, aromatic CH-2+CH-6), 141.35 (indolizine C-8a), 141.88 (aromatic C-4), 144.32 (indolizine C-2), 159.85 (CONH), 165.90 (COOEt). DEPT C^{135} (DMSO, 125 MHz, δ ppm): δ 14.71 (CH_3), 19.00 (indolizine CH_2-7), 22.75 (indolizine CH_2-8), 22.82 (indolizine CH_2-6), 45.84 (indolizine CH_2-5), 60.84 (OCH_2), 119.41 (2C, aromatic CH-3+CH-5), 130.49 (2C, aromatic CH-2+CH-6). MS (EI): m/z (%) 351 ($[M-H]^+$, 100%). Anal. Calcd. for $C_{19}H_{20}N_4O_3$ (352.39): C, 64.76; H, 5.72; N, 15.90. Found C, 65.13; H, 5.61; N, 15.54.

4.1.3.3. Ethyl 4-(2-amino-1-cyano-6,7,8,9-tetrahydro-5H-pyrrolo[1,2-a]azepine-3-carboxamido) benzoate (8c)

The title compound was prepared from the reaction of ethyl 4-(2-chloroacetamido)benzoate **7** (1.81 g, 7.5 mmol) with compound **5c** (1.21 g, 7.5 mmol) according to the general procedure B.

Compound **8b** was obtained as white solid product, m.p. 243-6 °C, yield 36%. IRυ_{max}/cm^{-1} 3268, 3164 (NHs), 3072, 3007 (C-H aromatic), 2932, 2869 (C-H aliphatic), 2212 (CN), 1706, 1667 (C=Os), 1465, 1436, 1364 (C-C, C-N). ^{1}H-NMR ($CDCl_3$, 500 MHz, δ ppm): δ 1.28 (t, 3H, J = 7.5 Hz, CH_3), 1.38-1.44 (m, 4H, pyrroloazepine CH_2-6+CH_2-8), 1.86-1.93 (m, 2H, pyrroloazepine CH_2-7), 2.94 (t, 2H, J = 5.6 Hz, pyrroloazepine CH_2-9), 4.35-4.44 (m, 4H, OCH_2 + pyrroloazepine CH_2-5), 4.62 (s, 2H, NH_2), 7.73 (d, 2H, J = 7.7 Hz, aromatic CH-3, CH-5), 8.01 (d, 2H, J = 7.7 Hz, aromatic CH-2, CH-6), 10.35 (s, H, CONH). ^{13}C-NMR ($CDCl_3$, 125 MHz, δ ppm): δ 14.33 (CH_3), 26.21 (pyrroloazepine CH_2-7), 26.64 (pyrroloazepine CH_2-9), 28.03 (pyrroloazepine CH_2-6), 30.52 (pyrroloazepine CH_2-8), 47.27 (pyrroloazepine CH_2-5), 61.27 (OCH_2), 83.05 (pyrroloazepine C-1), 116.02 (CN), 118.99 (2C, aromatic CH-3+CH-5), 125.55 (aromatic C-1), 129.29 (2C, aromatic CH-2+CH-6), 132.96 (pyrroloazepine C-3), 142.59 (pyrroloazepine C-9a), 143.13 (aromatic C-4), 149.49 (pyrroloazepine C-2), 159.23 (CONH), 165.64 (COOEt). DEPT C^{135} ($CDCl_3$, 125 MHz, δ ppm): δ 14.33 (CH_3), 26.21 (pyrroloazepine CH_2-7), 26.64 (pyrroloazepine CH_2-9), 28.03 (pyrroloazepine CH_2-6), 30.53 (pyrroloazepine CH_2-8), 47.26 (pyrroloazepine CH_2-5), 61.28 (OCH_2), 118.98 (2C, aromatic CH-3+CH-5), 129.29 (2C, aromatic CH-2+CH-6). MS (EI): m/z (%) 365 ([M-H]$^+$, 100). Anal. Calcd. for $C_{20}H_{22}N_4O_3$ (366.41): C, 65.56; H, 6.05; N, 15.29. Found C, 65.11; H, 5.74; N, 15.42.

4.1.4. General procedure (C) for preparation of compounds (9a,b)

A mixture of benzoate derivatives **8a**,**b** (3 mmol) and benzaldehyde (0.42 g, 4 mmol) in absolute ethanol (30 ml) in the presence of glacial acetic acid (0.5 ml) was refluxed for 6 hours. The reaction mixture was then concentrated, set aside to cool, where yellow/orange solid product was formed, collected and recrystallized from acetone-chloroform.

4.1.4.1. Ethyl 4-(6-(benzylideneamino)-7-cyano-2,3-dihydro-1*H*-pyrrolizine-5-carboxamido)benzoate (9a)

The title compound was prepared from the reaction of compound **8a** (1 g, 3 mmol) with benzaldehyde (0.42 g, 4 mmol) according to the general procedure C. Compound **9a** was obtained as yellow solid product, m.p. 246-9 °C, yield 64%. IRυ_{max}/cm^{-1} 3284, 3231 (NHs), 3058 (C-H

aromatic), 2990, 2909 (C-H aliphatic), 2218 (CN), 1714, 1672 (C=Os), 1594, 1545 (C=C, C=N), 1469, 1412, 1389, 1256 (C-N, C-O). ^{1}H-NMR ($CDCl_3$, 500 MHz, δ ppm): δ 1.33 (t, 3H, J = 7 Hz, CH_3), 2.51 (m, 2H, pyrrolizine CH_2-2), 3.00 (t, 2H, J = 7.5 Hz, pyrrolizine CH_2-1), 4.31 (q, 2H, J = 7 Hz, OCH_2), 4.48 (t, 2H, J = 7.2 Hz, pyrrolizine CH_2-3), 7.51 (m, 3H, aromatic CH-3+CH-4+CH-5), 7.67 (d, 2H, J = 10, aromatic protons), 7.88 (d, 2H, j = 7.5, aromatic protons), 7.98 (d, 2H, J = 7.5, aromatic protons), 9.13 (s, H, N=CH), 10.83 (s, H, CONH). ^{13}C NMR ($CDCl_3$, 125 MHz, δ ppm): δ 14.38 (CH_3), 24.60 (pyrrolizine CH_2-2), 25.45 (pyrrolizine CH_2-1), 50.18 (pyrrolizine CH_2-3), 60.80 (OCH_2), 115.99 (pyrrolizine C-7), 117.63 (CN), 118.68 (2C, aromatic CH-3+CH-5), 125.61 (pyrrolizine C-6), 128.76 (2C, aromatic CH-3+CH-5), 129.24 (2C, aromatic CH-2+CH-6), 130.92 (aromatic CH-2+CH-6), 132.65 (aromatic CH-4), 135.36 (aromatic C-1), 139.71 (pyrrolizine C-5), 142.50 (pyrrolizine C-7a), 145.32 (aromatic C-1), 148.56 (aromatic C-4), 158.61 (N=CH), 160.28 (CONH), 166.19 (COOEt). DEPT C^{135} ($CDCl_3$, 125 MHz, δ ppm): δ 14.38 (CH_3), 24.61 (indolizine CH_2-2), 25.46 (indolizine CH_2-1), 50.18 (indolizine CH_2-3), 60.81 (OCH_2), 118.68 (2C, aromatic CH-3+CH-5), 128.76 (2C, aromatic CH-3+CH-5), 129.24 (2C, aromatic CH-2+CH-6), 130.92 (aromatic CH-2+CH-6), 132.65 (aromatic CH-4). MS (EI): m/z (%) 426 (M^+, 100), Anal. Calcd. for $C_{25}H_{22}N_4O_3$ (426.47): C, 70.41; H, 5.20; N, 13.14. Found C, 69.97; H, 5.62; N, 13.38.

4.1.4.2. Ethyl 4-(2-(benzylideneamino)-1-cyano-5,6,7,8-tetrahydroindolizine-3-carboxamido)benzoate (9b)

The title compound was prepared from the reaction of compound **8b** (1.1 g, 3 mmol) with benzaldehyde (0.42 g, 4 mmol) according to the general procedure C. Compound **9b** was obtained as orange solid product, m.p. 251-4 °C, yield 57%. IRυ_{max}/cm^{-1} 3236, 3174 (NHs), 3059 (C-H aromatic), 2996, 2978, 2945 (C-H aliphatic), 2211 (CN), 1712, 1676 (C=Os), 1594, 1546 (C=C, C=N), 1410, 1317, 1277, 1258 (C-C, C-N). ^{1}H-NMR ($CDCl_3$, 500 MHz, δ ppm): δ 1.42 (t, 3H, J = 6.3 Hz, CH_3), 1.92 (m, 2H, indolizine CH_2-7), 2.04 (m, 2H, indolizine CH_2-6), 2.96 (t, 2H, J = 6.4 Hz, indolizine CH_2-8), 4.39 (q, 2H, J = 6.3 Hz, OCH_2), 4.55 (t, 2H, J = 6.7 Hz, indolizine CH_2-5′), 7.58 (m, 3H, aromatic CH-3+CH-4+CH-5), 7.72 (d, 2H, J = 7.6 Hz, aromatic CH-3+CH-5), 7.95 (d, 2H, J = 6.6 Hz, aromatic CH-2+CH-6), 8.04 (d. 2H, J = 7.5, aromatic CH-

2+CH-6), 9.15 (s, H, N=CH), 11.16 (s, H, CONH). ^{13}C-NMR ($CDCl_3$, 125 MHz, δ ppm): δ 14.41 (CH_3), 18.70 (indolizine CH_2-7), 22.93 (indolizine CH_2-8), 23.05 (indolizine CH_2-6), 47.08 (indolizine CH_2-5), 60.82 (OCH_2), 81.86 (indolizine C-1), 115.79 (CN), 118.73 (2C, aromatic CH-3+CH-5), 119.10 (indolizine C-2), 125.35 (aromatic C-1), 128.87 (2C, aromatic CH-3+CH-5), 129.24 (2C, aromatic CH-2+CH-6), 130.85 (2C, aromatic CH-2+CH-6), 132.76 (aromatic CH-4), 135.18 (indolizine C-3), 137.42 (indolizine C-8a), 142.71 (aromatic C-1), 143.38 (aromatic C-4), 159.15 (N=CH), 160.99 (CONH), 166.23 (COOEt). DEPT C^{135} ($CDCl_3$, 125 MHz, δ ppm): δ 14.41 (CH_3), 18.70 (indolizine CH_2-7), 22.93 (indolizine CH_2-8), 23.05 (indolizine CH_2-6), 47.07 (indolizine CH_2-5), 60.82 (OCH_2), 118.72 (2C, aromatic CH-3+CH-5), 128.87 (2C, aromatic CH-3+CH-5), 129.24 (2C, aromatic CH-2+CH-6), 130.85 (2C, aromatic CH-2+CH-6), 132.76 (aromatic CH-4). MS (EI): m/z (%) 439 ([M-H] $^+$, 6). Anal. Calcd. for $C_{26}H_{24}N_4O_3$ (440.49): C, 70.89; H, 5.49; N, 12.72. Found C, 71.32; H, 5.11; N, 12.42.

4.1.5. General procedure (D) for preparation of compounds 10a,b

A mixture of the carboxamide derivatives **8a**,**b** (3 mmol), benzoyl chloride (0.56 g, 4 mmol) and potassium carbonate (0.4 g, 3 mmol) in dichloromethane (DCM) was stirred for 24h at rt. The solvent was then evaporated, the solid residue was washed with aqueous $NaHCO_3$ and recrystallized from acetone-ethanol.

4.1.5.1. Ethyl 4-(6-benzamido-7-cyano-2,3-dihydro-1*H*-pyrrolizine-5-carboxamido)benzoate (10a)

The title compound was prepared from the reaction of compound **8a** (1 g, 3 mmol) with benzoyl chloride (0.56 g, 4 mmol) according to the general procedure D. Compound **10a** was obtained as white solid product, m.p. 249-52 °C, yield 55%. IRυ_{max}/cm^{-1} 3316, 3237 (NHs), 3030 (C-H aromatic), 2887, 2828 (C-H aliphatic), 2220 (CN), 1692, 1662 (C=Os), 1602, 1583, 1546 (C=C, C=N), 1454, 1427, 1327, 1282 (C-N, C-O). ^{1}H-NMR ($CDCl_3$, 500 MHz, δ ppm): δ 1.40 (t, 3H, J = 5 Hz, CH_3), 2.60 (m, 2H, pyrrolizine CH_2-2), 3.08 (t, 2H, J = 6.5 Hz, pyrrolizine CH_2-1), 4.37 (q, 2H, J = 6.6 Hz, OCH_2), 4.45 (t, 2H, J = 4.45 Hz, pyrrolizine CH_2-3), 7.57 (t, 2H, J = 7.7 Hz, aromatic CH-3+CH-5), 7.67 (m, 3H, aromatic CH-3+CH-5+CH-4), 8.01 (m, 4H, aromatic CH-

2+CH-6+CH-2+CH-6), 8.11 (s, H, Ph-NHCO), 10.19 (s, H, Ph-CONH). ^{13}C-NMR ($CDCl_3$, 125 MHz, δ ppm): δ 14.36 (CH_3), 25.12 (pyrrolizine CH_2-2), 25.67 (pyrrolizine CH_2-1), 49.68 (pyrrolizine CH_2-3), 60.85 (OCH_2), 84.65 (pyrrolizine C-7), 114.11 (CN), 118.72 (2C, aromatic CH-3+CH-5), 120.62 (aromatic C-1), 124.84 (pyrrolizine C-5), 125.92 (aromatic C-1), 127.70 (2C, aromatic CH-2+CH-6), 129.21 (2C, aromatic CH-3+CH-5), 130.81 (2C, aromatic CH-2+CH-6), 132.24 (pyrrolizine C-7a), 133.36 (aromatic CH-4), 142.23 (pyrrolizine C-6), 145.99 (aromatic C-4), 157.69 (CONH), 166.15 (NHCOPh), 169.24 (COOEt). DEPT C^{135} ($CDCl_3$, 125 MHz, δ ppm): δ 14.36 (CH_3), 25.12 (CH_2-2), 25.67 (CH_2-1), 49.69 (CH_2-3), 60.85 (OCH_2), 118.72 (2C, aromatic CH-3+CH-5), 127.70 (2C, aromatic CH-2+CH-6), 129.21 (2C, aromatic CH-3+CH-5), 130.81 (2C, aromatic CH-2+CH-6), 133.36 (aromatic CH-4). MS (EI): m/z (%) 456 ([(M+CH_3)-1]$^+$, 2). Anal. Calcd. for $C_{25}H_{22}N_4O_4$ (442.47): C, 67.86; H, 5.01; N, 12.66. Found C, 68.23; H, 4.72; N, 12.45.

4.1.5.2. Ethyl 4-(2-benzamido-1-cyano-5,6,7,8-tetrahydroindolizine-3-carboxamido)benzoate (10b)

The title compound was prepared from the reaction of compound **8b** (1.1 g, 3 mmol) with benzoyl chloride (0.56 g, 4 mmol) according to the general procedure D. Compound **10b** was obtained as white solid product, m.p. 261-4 °C, yield 57%. IRυ_{max}/cm^{-1} 3227, 3232 (NHs), 3057 (C-H aromatic), 2981, 2958, 2941 (C-H aliphatic), 2221 (CN), 1718, 1651 (C=Os), 1600, 1568, 1540, 1510 (C=C, C=N), 1441, 1278 (C-C, C-N). ^{1}H-NMR ($CDCl_3$, 500 MHz, δ ppm): δ 1.40 (t, 3H, J = 7.1 Hz, CH_3), 1.93 (m, 2H, indolizine CH_2-7), 2.02 (m, 2H, indolizine CH_2-6), 2.93 (t, 2H, J = 7.7 Hz, indolizine CH_2-8), 4.30 (t, 2H, J = 6.3 Hz, indolizine CH_2-5), 4.36 (q, 2H, J = 7.2 Hz, OCH_2), 7.54 (t, 2H, J = 6.9 Hz, aromatic CH-3+CH-5), 7.64 (t, H, J = 7.1 Hz, aromatic CH-4), 7.69 (d, 2H, J = 7.5 Hz, aromatic CH-3+CH-5), 7.99 (m, 3H, aromatic CH-2+CH-6+CONH), 8.12 (d, 2H, J = 7.8 Hz, aromatic CH-2+CH-6), 10.24 (s, H, Ph-NHCO). ^{13}C-NMR ($CDCl_3$, 125 MHz, δ ppm): δ 14.36 (CH_3), 18.92 (indolizine CH_2-7), 22.70 (indolizine CH_2-8), 22.84 (indolizine CH_2-6), 45.96 (indolizine CH_2-5), 60.87 (OCH_2), 88.98 (indolizine C-1), 114.05 (CN), 118.62 (2C, aromatic CH-3+CH-5), 122.14 (aromatic C-1), 123.90 (indolizine C-3), 125.95 (aromatic C-1), 127.71 (2C, aromatic CH-2+CH-6), 129.13 (2C, aromatic CH-3+CH-5), 130.79 (2C, aromatic CH-2+CH-6), 132.29 (aromatic CH-4), 133.24 (indolizine

C8a), 140.84 (indolizine C-2), 142.22 (aromatic C-4), 157.80 (PhNHCO), 166.15 (Ph-CONH), 169.59 (COOEt). DEPT C^{135} ($CDCl_3$, 125 MHz, δ ppm): δ 14.36 (CH_3), 18.93 (indolizine CH_2-7), 22.71 (indolizine CH_2-8), 22.84 (indolizine CH_2-6), 45.96 (indolizine CH_2-5), 60.87 (OCH_2), 118.62 (aromatic CH-3+CH-5), 127.71 (aromatic CH-2+CH-6), 129.13 (aromatic CH-3+CH-5), 130.79 (2C, aromatic CH-2+CH-6), 133.24 (aromatic CH-4). MS (EI): m/z (%) 455 ($[M-H]^+$, 100). Anal. Calcd. for $C_{26}H_{24}N_4O_4$ (456.49): C, 68.41; H, 5.30; N, 12.27. Found C, 67.96; H, 4.83; N, 11.87.

4.1.6. General procedure (E) for preparation of compounds (11a,b)

Preparation of compounds **11a**,**b** was achieved in two steps according to the previous report [26].

Preparation of the acid chloride of ibuprofen

A mixture of (±)-ibuprofen (1.22 g, 5.9 mmol) and thionyl chloride (1 gm, 8.41 mmol) was heated under reflux in water bath for 2 hours. The excess thionyl chloride was removed under reduced pressure and the residue (acid chloride) was dissolved in 40 ml DCM.

*Preparation of compounds **11a,b***

To the acid chloride solution obtained from ibuprofen, the carboxamides **8a,b** (3 mmol) and 0.5 ml of TEA were added. The reaction mixture was stirred at rt for two hours and left to stand overnight. The solvent was evaporated under reduced pressure. The remaining solid residue was washed two times with 10 mL of aqueous sodium carbonate 2% and left to dry. The solid product was recrystallized from ethanol-acetone

4.1.6.1. (±)-Ethyl 4-(7-cyano-6-(2-(4-isobutylphenyl)propanamido)-2,3-dihydro-1*H*-pyrrolizine-5-carboxamido)benzoate (11a)

The title compound was prepared from the reaction of compound **8a** (1 g, 3 mmol) with the acid chloride obtained from the reaction of thionyl chloride and ibuprofen (1.22 g, 5.9 mmol) according to the general procedure E. Compound **11a** was obtained as white solid product, m.p. 266-9 °C, yield 63%. IRυ_{max}/cm^{-1} 3397, 3279 (NHs), 2956, 2923, 2869 (C-H aliphatic), 2222 (CN), 1723, 1674 (C=Os), 1595, 1513 (C=C, C=N), 1492, 1467, 1317, 1277 (C-N, C-O). ^{1}H-NMR (DMSO-d_6, 500 MHz, δ ppm): 0.78 (d, 6H, J = 2.7 Hz, $CH(CH_3)_2$), 1.32 (t, 3H, J = 6.1 Hz, OCH_2CH_3), 1.44 (d, 3H, J = 6.1 Hz, Ph-$CHCH_3$), 1.71 (m, H, $CH(CH_3)_2$), 2.32 (d, 2H, J = 6.9 Hz, Ph-CH_2), 2.46 (m, 2H, pyrrolizine CH_2-2), 2.98 (t, 2H, J = 7.0 Hz, pyrrolizine CH_2-1), 3.91 (q, 1H, J = 6.2

Hz, Ph-$CHCH_3$), 4.28 (m, 4H, $COOCH_2$+ pyrrolizine CH_2-3), 6.98 (d, 2H, *J* = 7.0 Hz, aromatic CH-3+CH-5), 7.27 (d, 2H, *J* = 6.9 Hz, aromatic CH -2+ CH-6), 7.34 (d, 2H, *J* = 8.0 Hz, aromatic CH-3+CH-7), 7.85 (d, 2H, *J* = 7.9 Hz, aromatic CH-2+CH-6), 9.62 (s, H, NHCOCH), 10.26 (s, H, Ph-NHCO). ^{13}C-NMR (DMSO, 125 MHz, *δ* ppm): *δ* 14.68 (OCH_2CH_3), 18.85 (Ph-$CHCH_3$), 22.57, 22.58 ($CH(CH_3)_2$), 24.84 (pyrrolizine CH_2-2), 25.63 (pyrrolizine CH_2-1), 29.99 ($CH(CH_3)_2$), 44.71 (Ph-CH_2), 45.29 (Ph-$CHCH_3$), 49.76 (pyrrolizine CH_2-3), 60.93 (OCH_2CH_3), 84.75 (pyrrolizine C-7), 114.80 (CN), 118.57 (pyrrolizine C-5), 119.05 (2C, aromatic CH-3+CH-5), 124.97 (aromatic C-1), 127.24 (pyrrolizine C-7a), 127.53 (2C, aromatic CH-2+CH-6), 129.40 (2C, aromatic CH-3+CH-5), 130.56 (2C, aromatic CH-2+CH-6), 138.48 (aromatic C-1), 140.12 (aromatic C-4), 142.91 (aromatic C-4), 146.85 (pyrrolizine C-6), 157.84 (PhNHCO), 165.70 (COOEt), 175.29 (NHCOCH). DEPT C^{135} (DMSO, 125 MHz, *δ* ppm): *δ* 14.68 (OCH_2CH_3), 18.85 ($COCHCH_3$), 22.57 and 22.58 ($CH(CH_3)_2$), 24.84 (pyrrolizine CH_2-2), 25.63 (pyrrolizine CH_2-1), 29.99 ($CH(CH_3)_2$), 44.71 (Ph-CH_2), 45.29 (Ph-$CHCH_3$), 49.76 (pyrrolizine CH_2-3), 60.93 (OCH_2CH_3), 119.05 (2C, aromatic CH-3+CH-5), 127.53 (2C, aromatic CH-2+CH-6), 129.40 (2C, aromatic CH-3+CH-5), 130.56 (2C, aromatic CH-2+CH-6). MS (EI): m/z (%) 525 ([M-H] $^+$, 100). Anal. Calcd. for $C_{31}H_{34}N_4O_4$ (526.63): C, 70.70; H, 6.51; N, 10.64. Found C, 71.12; H, 6.67; N, 10.35.

4.1.6.2. (±)-Ethyl 4-(1-cyano-2-(2-(4-isobutylphenyl)propanamido)-5,6,7,8-tetrahydroindolizine-3-carboxamido)benzoate (11b)

The title compound was prepared from the reaction of compound **8b** (1.1 g, 3 mmol) with the acid chloride obtained from the reaction of thionyl chloride and ibuprofen (1.22 g, 5.9 mmol) according to the general procedure E. Compound **11b** was obtained as white solid product, m.p. 271-4 °C, yield 65%. IRυ_{max}/cm^{-1} 3404, 3287 (NHs), 2957, 2935, 2870 (C-H aliphatic), 2222 (CN), 1724, 1667 (C=Os), 1596, 1537, 1518 (C=C, C=N), 1491, 1365, 1280 (C-C, C-N). ^{1}H-NMR ($CDCl_3$, 500 MHz, *δ* ppm): *δ* 0.88 (d, 6H, *J* = 5.4 Hz, $CH(CH_3)_2$), 1.43 (t, 3H, *J* = 5.2 Hz, OCH_2CH_3), 1.65 (d, 3H, *J* = 5.0 Hz, Ph-$CHCH_3$), 1.81 (m, H, $CH(CH_3)_2$), 1.88 (m, 2H, indolizine CH_2-7), 1.98 (m, 2H, indolizine CH_2-6), 2.42 (d, 2H, *J* = 6.0 Hz, Ph-CH_2), 2.87 (t, 2H, *J* = 6.5 Hz, indolizine CH_2-8), 3.84 (q, H, *J* = 6.8 Hz, Ph-$CHCH_3$), 4.17 (t, H, *J* = 7.5 Hz, indolizine CH_2-5), 4.27 (t, H, *J* = 7.5 Hz, CH_2-5), 4.39 (q, 2H, *J* = 5.8 Hz, OCH_2CH_3), 7.05 (d, 2H, *J* = 6.2 Hz, aromatic CH-3+CH-5), 7.21 (d, 2H, *J* = 6.1 Hz, aromatic CH-2+CH-6), 7.39 (s,

H, NHCOCH), 7.54 (d, 2H, *J* = 7.5 Hz, aromatic CH-3+CH-5), 7.98 (d, 2H, *J* = 7.6 Hz, aromatic CH-2+CH-6), 9.84 (s, H, Ph-NHCO). ^{13}C-NMR ($CDCl_3$, 125 MHz, δ ppm): δ 14.40 (OCH_2CH_3), 18.08 (Ph-$CHCH_3$), 18.89 (indolizine CH_2-7), 22.35, 22.37 ($CH(CH_3)_2$), 22.67 (indolizine CH_2-8), 22.74 (indolizine CH_2-6), 30.11 ($CH(CH_3)_2$), 44.95 ($PhCH_2$), 45.81 (indolizine CH_2-5), 46.80 (Ph-$CHCH_3$), 60.86 (OCH_2CH_3), 88.74 (indolizine C-1), 113.70 (CN), 118.68 (2C, aromatic CH-3+CH-5), 122.20 (indolizine C-3), 123.34 (aromatic C-1), 125.86 (indolizine C-8a), 127.40 (2C, aromatic CH-2+CH-6), 129.98 (2C, aromatic CH-3+CH-5), 130.68 (2C, aromatic CH-2+CH-6), 136.40 (aromatic C-1), 140.67 (aromatic C-4), 141.60 (aromatic C-4), 142.07 (indolizine C-2), 157.74 (PhNHCO), 166.19 (COOEt), 177.51 (NHCOCH). DEPT C^{135} ($CDCl_3$, 125 MHz, δ ppm): δ 14.40 (OCH_2CH_3), 18.09 ($OCHCH_3$), 18.89 (indolizine CH_2-7), 22.35, 22.37 ($CH(CH_3)_2$), 22.67 (indolizine CH_2-8), 22.75 (indolizine CH_2-6), 30.12 ($CH(CH_3)_2$), 44.95 ($PhCH_2$), 45.81 (indolizine CH_2-5), 46.79 (Ph-$CHCH_3$), 60.87 (OCH_2CH_3), 118.68 (2C, aromatic CH-3+CH-5), 127.40 (2C, aromatic CH-2+CH-6), 129.98 (2C, aromatic CH-3+CH-5), 130.68 (2C, aromatic CH-2+CH-6). MS (EI): m/z (%) 554 554 ($[(M+CH_3)-1]^+$, 4). Anal. Calcd. for $C_{32}H_{36}N_4O_4$ (540.65): C, 71.09; H, 6.71; N, 10.36. Found C,70.82; H, 6.34; N, 10.61.

4.1.7. Diethyl 4,4'-((6,6'-(oxalylbis(azanediyl))bis(7-cyano-2,3-dihydro-1H-pyrrolizine-5,5'-carbonyl))bis(azanediyl))dibenzoate (12)

A solution of compound **8a** (1 g, 2.96 mmol) in 50 mL DCM was added dropwise with stirring to a solution of oxalyl chloride (1 g, 8 mmol) in 30 mL DCM. The reaction mixture was stirred for 4h at room temperature. The solvent was evaporated under reduced pressure. The solid product was washed three times with acetone (20 mL). Compound **12** was obtained as white solid, m.p. 336-9 °C, yield 44%, IRυ_{max}/cm^{-1} 3398, 3328 (NHs), 3073, 3044 (C-H aromatic), 2902, 2833 (C-H aliphatic), 2212 (CN), 1707, 1667 (C=O), 1603, 1510 (C=C, C=N), 1423, 1365, 1310, 1279 (C-C, C-N). ^{1}H-NMR (DMSO-d_6, 500 MHz, δ ppm): δ 1.32 (t, 6H, *J* = 7.1 Hz, CH_3+CH_3), 2.47 (m, 4H, pyrrolizine CH_2-2+CH_2-2), 3.01 (t, 4H, *J* = 7.4 Hz, pyrrolizine CH_2-1+CH_2-1), 4.28-4.32 (m, 8H, pyrrolizine CH_2-3+CH_2-3+ ester OCH_2+OCH_2), 7.78 (d, 4H, *J* = 8.7 Hz, aromatic CH-3+CH-5+ CH-3+CH-5), 7.95 (d, 4H, *J* = 8.7 Hz, aromatic CH-2+CH-6+ CH-2+CH-6), 9.87 (s, 2H, Ph-NHCO) 10.78 (s, 2H, CONH+CONH′). ^{13}C-NMR (DMSO, 125 MHz, δ ppm): δ 14.69

(CH_3+CH_3), 24.84 (pyrrolizine CH_2-2+CH_2-2), 25.71 (pyrrolizine CH_2-1+CH_2-1), 49.79 (pyrrolizine CH_2-3+CH_2-3), 60.99 (OCH_2+OCH_2), 84.64 (pyrrolizine C-7+C-7), 114.92 (CN+CN), 117.55 (aromatic C-1+C-1), 119.81 (aromatic CH-3+CH-5+CH-3+CH-5), 125.09 (pyrrolizine C-5+C-5), 126.86 (pyrrolizine C-7a+C-7a), 130.59 (aromatic CH-2+CH-6+CH-2+CH-6), 143.49 (pyrrolizine C-6+C-6), 147.02 (aromatic C-4+C-4), 158.14 (CONH+CONH), 161.69 (two COOEt), 165.80 (COCO). DEPT C^{135} (DMSO, 125 MHz, δ ppm): δ 14.69 (CH_3+CH_3), 24.84 (pyrrolizine CH_2-2+CH_2-2), 25.71 (pyrrolizine CH_2-1+CH_2-1), 49.79 (pyrrolizine CH_2-3+CH_2-3), 60.99 (OCH_2+OCH_2), 119.81 (aromatic CH-3+CH-5+CH-3+CH-5), 130.59 (aromatic CH-2+CH-6+CH-2′+CH-6). MS (EI): m/z (%) 731 ($[M+H]^+$, 3%), 729 ($[M-H]^+$, 2%). Anal. Calcd. for $C_{38}H_{34}N_8O_8$ (730.73): C, 62.46; H, 4.69; N, 15.33; Found C,62.88; H, 4.43; N, 15.83.

4.2. Biological evaluation

4.2.1. Animals

Sprague-Dawley rats (both sex, 200-250g) and albino mice (both sex, 25-35g) were used in evaluation of anti-inflammatory and analgesic activities, respectively. the animals were acquired from animal house of Medical Research Centre, King Abdul-Aziz University, Jeddah, Kingdom of Saudi Arabia. The animals were housed arbitrarily and spread to treatment groups in polypropylene cages bedded with wooden husk. They were kept in optimal condition (food and tap water *ad libitum*, 12/12 h light/dark cycle). Experimental methods and protocols used in this study were reviewed by the Institutional Review Board Committee and were in agreement with the guidelines.

4.2.2. Anti-Inflammatory Activity.

In this study, carrageenan-induced rat paw edema model was used to evaluate the anti-inflammatory activity of compounds **8-11** according to the previous report [31]. The rats were divided randomly into ten groups (control, standard and 8 groups for test compounds, n = 6). Rats were uniformly hydrated to reduce variability to edema response. The animals in each

group received the specified test compound (ibuprofen or compounds **8-11**) at a dose of 0.48 mmol/kg p.o. Ibuprofen and test compounds were prepared as suspension in saline (0.9% NaCl) containing 5 drops of 0.5% carboxymethyl cellulose (CMC). The control group received the same volume of vehicle (saline containing 5 drops of 0.5% CMC). The % inhibition of edema thickness caused by test compound and ibuprofen were used as a measure of their anti-inflammatory activity. The anti-inflammatory activity of test compounds were calculated using the formula: anti-inflammatory activity = $(1-L_t/L_c) \times 100$; where L_t is the mean change in paw diameter in rats treated with the tested compounds; L_c is the mean increase in paw diameters in control group. The anti-inflammatory activity were calculated at 2 and 4 h post carrageenan administration. The results were presented in **Fig. 3** and **Table 1**.

4.2.3. Analgesic activity

4.2.3.1. Hot plate test

The albino mice were randomly divided into 11 groups (n = 6). Nine of these groups received the test compounds **8-11** (0.48 mmol/kg), one group (control) received normal saline and the last group received ibuprofen (100 mg/kg) orally. The anti-nociceptive activity of test compounds was assessed by hot plate test [26,30] to evaluate the pain-relieving property. Animals were placed individually onto a hot plate with temperature fixed at 55+ 0.5°C (Harvard Apparatus Ltd., Kent, UK). Each mouse represented as its own control. The latency time (period taken by the individual mouse to react by licking the forepaws or jumping) was determined as the response. Early latency (pretreatment value) was determined just before giving normal saline/ibuprofen/test compounds for each mouse. The withdrawal latency was determined at 2h and 4h after the injection of saline/ibuprofen/test compounds. The extension in the withdrawal latency was taken as an index for the analgesic effect. The results were summarized in **Table 2**.

4.2.3.2. Acetic acid induced writhing test

Acetic acid induced writhing test was used to evaluate the analgesic activity of compounds **8-11** according to our previous report [22]. Grouping and other conditions were essentially like those described in hot plate test (n = 6). The mice received ibuprofen, test compounds or saline at a dose of 0.48 mmol/kg/day. Abdominal writhing was induced by acetic acid (0.6%) at 4h after

administration of test compounds. The number of writhes were recorded for each mouse until 30 min. The results were presented in **Table 3**.

4.2.4. Acute ulcerogenicity studies

In this study, adult rats of both sexes weighing between 200-250 g were divided into ten groups (n = 6). The rats were fasted for 20 hours before administration of test compounds. The first (control) group received normal saline containing 5 drops of CMC. The remaining groups received Ibuprofen/test compounds **8-11** at a dose of 0.48 mmol/kg/day (p.o.). After administration of test compounds, rats are fasted for 2 h, then allowed feed for another 2 h followed by fasting for 20 h. two additional doses are given to the rats in the second and third day. Rats were sacrificed in the fourth day and stomachs were removed, opened and examined using magnifying lens (10x). the number of mucosal damages and their scores were determined according to the previous report [22]. The results were presented in **Table 1**.

4.2.5. Histopathological studies

The stomachs of the rats used in the acute ulcerogenic studies were fixed for 72 h in formalin solution (10%). The specimens were treated according to our previous report [26]. Tissue sections (5 microns thick) were prepared using Microtome. The cross sections were examined after Haematoxylin and Eosin stain. The results were presented in **Figs. 4** and **5**.

4.2.6. *In vitro* COX-1/2 inhibitory assay

The ability of compounds **8-10** to inhibit COX-1 (human, Item No. 701070) and COX-2 (human, Item No. 701080) enzymes *in vitro* was measured using COX inhibitor assay kit provided from Cayman Chemicals. The assay was done according to manufacturer's instructions and as mentioned before [32]. The results were represented in **Table 4**.

4.2.7. Cytotoxic activity

4.2.7.1. Cell culture

In this study, the cytotoxic activity of compounds **8-11** were evaluated against MCF-7 breast, A2780 ovarian, HT29 colon cancer cell lines. In addition, their cytotoxic effects were also

evaluated against MRC5 normal non transformed fibroblast cell line was also used. The cell culture medium and growth conditions were as previously reported [30].

4.2.7.2. Cytotoxicity assay

The MTT assay was used in the evaluation of cytotoxic activity of compounds **8-11** according to our previous reports [34,35]. The cells lines were cultured in 96-well plates for 72 h. Briefly, cells were seeded in 96-well plates for 24 h. The cells were then treated with compounds 8-11 in Dulbecco's modified Eagles medium /F-12 medium DMEM/F12 supplemented with 5% fetal bovine serum (FBS). After treatment with test compounds for 72 h, cancer cells were incubated with MTT (0.5 mg/mL) for 3h. The absorbance of the purple formazan was determined using multi-plate reader at 570 nm. The IC_{50} values of each compound was determined using Graph Pad Prism version 5.00 for Windows was used for analysis. Results were presented in **Table 5**.

4.2.8. Cell cycle analysis

The effect of compound **9a** on the cell cycle perturbations of MCF-7 cells was determined according to our previous report [35]. Briefly, after overnight seeding of MCF-7 cells into 6 well plates, the cells were incubated with compound **9a** at 0, 0.1, 0.5 and 1 μM for 24 h. after incubation, cells were washed with the ice-cold phosphate buffer, then cells were incubated for 5 min with trypsin (0.5 mL). The experimental procedures were completed according to our previous report [35]. Cells were treated for 24 h with compound **9a** at 0, 0.1, 0.5 and 1 μM. Cell cycle analysis of MCF-7 was performed according to our previous report [35]. The results were summarized in **Table 6** and **Fig. 8**.

4.2.9. Annexin V-FITC/PI apoptosis assay

The ability of compound **9a** to induce apoptosis in MCF-7 cells was evaluated using Annexin V-FITC/PI staining [30,34]. Briefly, after overnight seeding of MCF-7 cells into 6 well plates, the cells were treated with compound **9a** at 0, 0.1, 0.5 and 1 μM for 24 h. Microscopical examination was performed before and after the treatment with test compound to detect any morphological changes. The experimental procedures were completed according to our previous reports [30,34]. Different cell populations including early apoptotic, late apoptotic, and necrotic cells were

determined based on annexin V and PI staining. The analysis was done by NovoCyte Flow Cytometer, Acea Biosciences Inc., California, USA). The results were presented in **Figs. 9** and **10**.

4.3. Computational studies

4.3.1. Molecular docking studies

A molecular docking study was performed to investigate the binding modes of compounds **8-11** into the active site of COX-1/2. The pdb files of COX-1 (pdb code: 1EQG) [39] and COX-2 (pdb code: 1CX2) [40], were downloaded from protein data bank (http://www.rcsb.org/pdb). The study was performed using AutoDock 4.2 [38]. The ligands, enzymes, affinity map, grid and docking parameter files were prepared according to our previous reports [41,42]. The results were summarized in **Tables 7** and **8**. Visualization of 2/3D binding modes of the new compounds into COX-1/2 was done using LigPlot^{+} [43] and discovery studio visualizer [44].

4.3.2. Drug-likeness and ADME studies

The physicochemical properties (MW, MlogP, H_D, H_A, TPSA, and number of rotatable bonds) which affect pharmacokinetics (ADME) of the new compounds **8-11** were determined using SwissADME webserver (http://www.swissadme.ch/) [47]. The first step (input) started with using the molecular sketcher to draw chemical structure of the new compounds. The chemical structures were transferred to SMILES list (Table S5, supplementary data). The webserver start ADME calculations by clicking "Run" button. The molecular volume and drug-likeness score (DLS) of the new compounds were calculated using Molsoft webserver (http://molsoft.com/mprop/). The webserver is provided with molecular editor to draw the chemical structures of the new compounds and calculations start by clicking on the "calculate properties" button. The results were summarized in **Tables 9**.

Acknowledgement

The authors would like to thank the Institute of Scientific Research and Revival of Islamic Heritage, Umm Al-Qura University, Makkah, Saudi Arabia for their continuous support. This work was supported financially by the Institute of Scientific Research and Revival of Islamic Heritage, Umm Al-Qura University, Makkah, Saudi Arabia to Dr. Khalid Mahmoud Attalah (Grant No: 43310014).

Supplementary data

Supplementary data including all spectral data and copies of IR, Mass, ^{1}H-NMR and ^{13}C-NMR spectra, of all final compounds was provided with this manuscript.

Conflict of Interest

Authors declared that there is no conflict of interest and have approved the article.

5. References

1. F.R. Balkwill, A. Mantovani, Cancer-related inflammation: common themes and therapeutic opportunities., Semin. Cancer Biol. 22 (2012) 33–40. doi:10.1016/j.semcancer.2011.12.005.
2. A.M. Cipta, C.J. Pietras, T.E. Weiss, T.B. Strouse, Cancer-related pain management in clinical oncology., J. Community Support. Oncol. 13 (2015) 347–355. doi:10.12788/jcso.0173.
3. L.M. Coussens, Z. Werb, Inflammation and cancer, Nature. 420 (2002) 860–867. doi:10.1038/nature01322.
4. A.J. Schetter, N.H.H. Heegaard, C.C. Harris, Inflammation and cancer: interweaving microRNA, free radical, cytokine and p53 pathways., Carcinogenesis. 31 (2010) 37–49. doi:10.1093/carcin/bgp272.
5. R.E. Harris, B.C. Casto, Z.M. Harris, Cyclooxygenase-2 and the inflammogenesis of breast cancer., World J. Clin. Oncol. 5 (2014) 677–692. doi:10.5306/wjco.v5.i4.677.
6. H. Sun, X. Zhang, D. Sun, X. Jia, L. Xu, Y. Qiao, Y. Jin, COX-2 expression in ovarian cancer: an updated meta-analysis., Oncotarget. 8 (2017) 88152–88162. doi:10.18632/oncotarget.21538.
7. H.M.J. Roelofs, R.H.M. Te Morsche, B.W.H. van Heumen, F.M. Nagengast, W.H.M. Peters, Over-expression of COX-2 mRNA in colorectal cancer., BMC Gastroenterol. 14 (2014) 1. doi:10.1186/1471-230X-14-1.
8. C. Sobolewski, C. Cerella, M. Dicato, L. Ghibelli, M. Diederich, The role of cyclooxygenase-2 in cell proliferation and cell death in human malignancies., Int. J. Cell Biol. 2010 (2010) 215158. doi:10.1155/2010/215158.
9. A.T. Koki, J.L. Masferrer, Celecoxib: a specific COX-2 inhibitor with anticancer properties., Cancer Control. 9 (2002) 28–35. doi:10.1177/107327480200902S04.
10. T. Kitamura, T. Kawamori, N. Uchiya, M. Itoh, T. Noda, M. Matsuura, T. Sugimura, K. Wakabayashi, Inhibitory effects of mofezolac, a cyclooxygenase-1 selective inhibitor, on intestinal carcinogenesis., Carcinogenesis. 23 (2002) 1463–1466. https://doi.org/10.1093/carcin/23.9.1463
11. A.M. Gouda, E.A. Beshr, F.A. Almalki, H. Hisham, B. Fawzi Taj, A. Faiz Alnafaei, R. Sulaiman Alharazi, W. Mahmood kazi, M.M. AlMatrafi, Arylpropionic acid-derived NSAIDs: New insights on derivatization, anticancer activity and potential mechanism of action, Bioorg. Chem. 92 (2019) 103224. doi:https://doi.org/10.1016/j.bioorg.2019.103224.

12. E. Gurpinar, W.E. Grizzle, G.A. Piazza, NSAIDs inhibit tumorigenesis, but how?, Clin. Cancer Res. 20 (2014) 1104–1113. doi:10.1158/1078-0432.CCR-13-1573.
13. A.M. Gouda, A.H. Abdelazeem, An integrated overview on pyrrolizines as potential anti-inflammatory, analgesic and antipyretic agents., Eur. J. Med. Chem. 114 (2016) 257–292. doi:10.1016/j.ejmech.2016.01.055.
14. J.C. Becker, W. Domschke, T. Pohle, Current approaches to prevent NSAID-induced gastropathy - COX selectivity and beyond, Br. J. Clin. Pharmacol. 58 (2004) 587–600. doi:10.1111/j.1365-2125.2004.02198.x.
15. C. Vidal, A. Gomez-Hernandez, E. Sanchez-Galan, A. Gonzalez, L. Ortega, J.A. Gomez-Gerique, J. Tunon, J. Egido, Licofelone, a balanced inhibitor of cyclooxygenase and 5-lipoxygenase, reduces inflammation in a rabbit model of atherosclerosis., J. Pharmacol. Exp. Ther. 320 (2007) 108–116. doi:10.1124/jpet.106.110361.
16. W. Liu, J. Zhou, K. Bensdorf, H. Zhang, H. Liu, Y. Wang, H. Qian, Y. Zhang, A. Wellner, G. Rubner, W. Huang, C. Guo, R. Gust, Investigations on cytotoxicity and anti-inflammatory potency of licofelone derivatives, Eur. J. Med. Chem. 46 (2011) 907–913. doi:10.1016/j.ejmech.2011.01.002.
17. S. Tavolari, M. Bonafe, M. Marini, C. Ferreri, G. Bartolini, E. Brighenti, S. Manara, V. Tomasi, S. Laufer, T. Guarnieri, Licofelone, a dual COX/5-LOX inhibitor, induces apoptosis in HCA-7 colon cancer cells through the mitochondrial pathway independently from its ability to affect the arachidonic acid cascade., Carcinogenesis. 29 (2008) 371–380. doi:10.1093/carcin/bgm265.
18. N.K. Narayanan, D. Nargi, M. Attur, S.B. Abramson, B.A. Narayanan, Anticancer effects of licofelone (ML-3000) in prostate cancer cells., Anticancer Res. 27 (2007) 2393–2402.
19. A.M. Gouda, A.H. Abdelazeem, H.A. Omar, A.N. Abdalla, M.A.S. Abourehab, H.I. Ali, Pyrrolizines: design, synthesis, anticancer evaluation and investigation of the potential mechanism of action, Bioorg. Med. Chem. 25 (2017) 5637–5651. doi:https://doi.org/10.1016/j.bmc.2017.08.039.
20. S.K. Joishy, D. Walsh, The opioid-sparing effects of intravenous ketorolac as an adjuvant analgesic in cancer pain: application in bone metastases and the opioid bowel syndrome., J. Pain Symptom Manage. 16 (1998) 334–339. https://doi.org/10.1016/S0885-3924(98)00081-5.
21. B.C.Q. Nguyen, H. Takahashi, Y. Uto, M.D. Shahinozzaman, S. Tawata, H. Maruta, 1,2,3-Triazolyl ester of Ketorolac: A “Click Chemistry”-based highly potent PAK1-blocking cancer-killer., Eur. J. Med. Chem. 126 (2017) 270–276. doi:10.1016/j.ejmech.2016.11.038.
22. S.E. Abbas, F.M. Awadallah, N.A. Ibrahim, A.M. Gouda, Novel substituted and fused pyrrolizine derivatives: Synthesis, anti-inflammatory and ulcerogenecity studies, Eur. J. Med. Chem. 45 (2010) 482–491. doi:10.1016/j.ejmech.2009.10.031.
23. P.K. Halen, P.R. Murumkar, R. Giridhar, M.R. Yadav, Prodrug designing of NSAIDs., Mini Rev. Med. Chem. 9 (2009) 124–139. DOI: 10.2174/138955709787001695.
24. C. Luong, A. Miller, J. Barnett, J. Chow, C. Ramesha, M.F. Browner, Flexibility of the NSAID binding site in the structure of human cyclooxygenase-2., Nat. Struct. Biol. 3 (1996) 927–933.

25. A.S. El-Azab, A.A.-M. Abdel-Aziz, L.A. Abou-Zeid, W.M. El-Husseiny, A.M. El Morsy, M.A. El-Gendy, M.A.-A. El-Sayed, Synthesis, antitumour activities and molecular docking of thiocarboxylic acid ester-based NSAID scaffolds: COX-2 inhibition and mechanistic studies., J. Enzyme Inhib. Med. Chem. 33 (2018) 989–998. doi:10.1080/14756366.2018.1474878.
26. A.M. Gouda, H.I. Ali, W.H. Almalki, M.A. Azim, M.A.S. Abourehab, A.H. Abdelazeem, Design, Synthesis, and Biological Evaluation of Some Novel Pyrrolizine Derivatives as COX Inhibitors with Anti-Inflammatory/Analgesic Activities and Low Ulcerogenic Liability., Molecules. 21 (2016) 1-21. doi:10.3390/molecules21020201.
27. A. Belal, A.M. Gouda, A.S. Ahmed, N.M. Abdel Gawad, Synthesis of novel indolizine, diazepinoindolizine and Pyrimidoindolizine derivatives as potent and selective anticancer agents, Res. Chem. Intermed. 41 (2015) 9687–9701. doi:10.1007/s11164-015-1958-9.
28. S.E. Abbas, F.M. Awadallah, N.A. Ibrahim, A.M. Gouda, B.A. Shehata, Design, synthesis and preliminary evaluation of some novel [1,4]diazepino [5,6-b]pyrrolizine and 6-(2-oxopyrrolidino)-1H-pyrrolizine derivatives as anticonvulsant agents, Med. Chem. Res. 20 (2011) 1015–1023. doi:10.1007/s00044-010-9429-8.
29. K.M. Attallah, A.M. Gouda, I.T. Ibrahim, L. Abouzeid, Design, synthesis, 99mTc labeling, and biological evaluation of a novel pyrrolizine derivative as potential anti-inflammatory agent, Radiochemistry. 59 (2017) 630–638. doi:10.1134/S10663622170600121.
30. A.M. Gouda, A.H. Abdelazeem, A.N. Abdalla, M. Ahmed, Pyrrolizine-5-carboxamides: Exploring the impact of various substituents on anti-inflammatory and anticancer activities, Acta Pharm. 68 (2018) 251–273. doi:https://doi.org/10.2478/acph-2018-0026.
31. C.A. Winter, E.A. Risley, G.W. Nuss, Carrageenin-induced edema in hind paw of the rat as an assay for antiiflammatory drugs., Proc. Soc. Exp. Biol. Med. 111 (1962) 544–547. doi: 10.3181/00379727-111-27849.
32. S.-Z. Ren, Z.-C. Wang, D. Zhu, X.-H. Zhu, F.-Q. Shen, S.-Y. Wu, J.-J. Chen, C. Xu, H.-L. Zhu, Design, synthesis and biological evaluation of novel ferrocene-pyrazole derivatives containing nitric oxide donors as COX-2 inhibitors for cancer therapy, Eur. J. Med. Chem. 157 (2018) 909–924. doi:https://doi.org/10.1016/j.ejmech.2018.08.048.
33. M.T. Elsaady, A.M. Gouda, F.H. Edrees, N.M.A. Gawad, synthesis and biological evaluation of some novel Schiff base derivatives as potential anticancer agents, J Chem. Pharm. Res. 8 (2016) 273–282.
34. W.H. Malki, A.M. Gouda, H.E.A. Ali, R. Al-Rousan, D. Samaha, A.N. Abdalla, J. Bustamante, Z.Y. Abd Elmageed, H.I. Ali, Structural-based design, synthesis, and antitumor activity of novel alloxazine analogues with potential selective kinase inhibition, Eur. J. Med. Chem. 152 (2018) 31–52. doi:https://doi.org/10.1016/j.ejmech.2018.04.029.
35. A.M. Gouda, H.A. El-Ghamry, T.M. Bawazeer, T.A. Farghaly, A.N. Abdalla, A. Aslam, Antitumor activity of pyrrolizines and their Cu(II) complexes: Design, synthesis and cytotoxic screening with potential apoptosis-inducing activity., Eur. J. Med. Chem. 145 (2018) 350–359. doi:10.1016/j.ejmech.2018.01.009.
36. L.M. Zuckerman, W.L. Frames, J.G. Elsissy, T.G. Shields, R. de Necochea-Campion, H.R. Mirshahidi, N.L. Williams, S. Mirshahidi, The effect of non-steroidal anti-inflammatory

drugs on osteosarcoma cells., Eur. Rev. Med. Pharmacol. Sci. 23 (2019) 2681–2690. doi:10.26355/eurrev_201903_17416.
37. J.N. Cashman, The mechanisms of action of NSAIDs in analgesia., Drugs. 52 Suppl 5 (1996) 13–23. doi:10.2165/00003495-199600525-00004.
38. G.M. Morris, R. Huey, W. Lindstrom, M.F. Sanner, R.K. Belew, D.S. Goodsell, A.J. Olson, AutoDock4 and AutoDockTools4: Automated docking with selective receptor flexibility, J. Comput. Chem. 30 (2009) 2785–2791. doi:10.1002/jcc.21256.
39. B.S. Selinsky, K. Gupta, C.T. Sharkey, P.J. Loll, Structural analysis of NSAID binding by prostaglandin H2 synthase: time-dependent and time-independent inhibitors elicit identical enzyme conformations, Biochemistry. 40 (2001) 5172–5180. doi:10.1021/bi010045s.
40. R.G. Kurumbail, A.M. Stevens, J.K. Gierse, J.J. McDonald, R.A. Stegeman, J.Y. Pak, D. Gildehaus, J.M. Miyashiro, T.D. Penning, K. Seibert, P.C. Isakson, W.C. Stallings, Structural basis for selective inhibition of cyclooxygenase-2 by anti-inflammatory agents, Nature. 384 (1996) 644–648. doi:10.1038/384644a0.
41. A.M. Gouda, F.A. Almalki, Carprofen : a theoretical mechanistic study to investigate the impact of hydrophobic interactions of alkyl groups on modulation of COX - 1/2 binding selectivity, SN Appl. Sci. 1 (2019). https://doi.org/10.1007/s42452-019-0335-5.
42. F.A. Almalki, A.M. Gouda, M.H. Bin Ali, O.M. Almehmadi, Profens: a comparative molecular docking study into cyclooxygenase-1/2, Drug Invent Today 11 (2019) 480–487.
43. R.A. Laskowski, M.B. Swindells, LigPlot+: multiple ligand-protein interaction diagrams for drug discovery, J. Chem. Inf. Model. 51 (2011) 2778–2786. doi:10.1021/ci200227u.
44. Dassault systems BIOVIA, Discovery Studio Visualizer, v16.1.0.15350, San Diego: Dassault systems, (2016).
45. B. Seruga, A. Ocana, E. Amir, I.F. Tannock, Failures in Phase III: Causes and Consequences., Clin. Cancer Res. 21 (2015) 4552–4560. doi:10.1158/1078-0432.CCR-15-0124.
46. D.L. Jardim, E.S. Groves, P.P. Breitfeld, R. Kurzrock, Factors associated with failure of oncology drugs in late-stage clinical development: A systematic review., Cancer Treat. Rev. 52 (2017) 12–21. doi:10.1016/j.ctrv.2016.10.009.
47. A. Daina, O. Michielin, V. Zoete, SwissADME: a free web tool to evaluate pharmacokinetics, drug-likeness and medicinal chemistry friendliness of small molecules., Sci. Rep. 7 (2017) 42717. doi:10.1038/srep42717.
48. C.A. Lipinski, F. Lombardo, B.W. Dominy and P. J. Feeney, Experimental and computational approaches to estimate solubility and permeability in drug discovery and development settings, Adv. Drug. Deliver. Rev. 23 (1997) 3–25; https://doi.org/10.1016/S0169-409X(96)00423-1.
49. Y.H. Zhao, M.H. Abraham, J. Le, A. Hersey, C.N. Luscombe, G. Beck, B. Sherborne, I. Cooper, Rate-limited steps of human oral absorption and QSAR studies., Pharm. Res. 19 (2002) 1446–1457. doi:10.1023/a:1020444330011.

List of abbreviations

ACD, arachidonic acid; ADT, The AutoDock Tool; $CDCl_3$, deuterated chloroform; CMC, carboxymethyl cellulose; COX-1/2, cyclooxygenase-1/2; DCM, dichloromethane (methylene chloride); DEPT, distortionless enhancement by polarization transfer; $\Delta G_{b,}$ binding free energy; DMSO, dimethyl sulfoxide; DMEM/F12, Dulbecco's modified Eagles medium /F-12 medium; FBS, fetal bovine serum; FITC, fluorescein isothiocyanate; GIT, gastrointestinal tract; IC_{50}, half maximal inhibitory concentration; IR, infrared; K_i, inhibition constants; 5-LOX, 5-lipoxygenase; MTT, 3-(4,5-dimethylthiazol-2-yl)-2,5-diphenyl-2H-tetrazolium bromide; NSAIDs, nonsteroidal anti-inflammatory drugs; PI, propidium iodide; RMSD, root mean square deviation; SAR, structure activity relationship; SI, selectivity index.

Declaration of interests

☒ The authors declare that they have no known competing financial interests or personal relationships that could have appeared to influence the work reported in this paper.

☐The authors declare the following financial interests/personal relationships which may be considered as potential competing interests: